

Online Rack Placement in Large-Scale Data Centers

Saumil Baxi

Cloud Operations and Innovation, Microsoft

Kayla Cummings

Cloud Supply Chain Sustainability Engineering, Microsoft

Alexandre Jacquillat, Sean Lo

Sloan School of Management, Operations Research Center, Massachusetts Institute of Technology

Rob McDonald

Cloud Operations and Innovation, Microsoft

Konstantina Mellou, Ishai Menache, Marco Molinaro

Machine Learning and Optimization, Microsoft Research

This paper optimizes the configuration of large-scale data centers toward cost-effective, reliable and sustainable cloud supply chains. We formulate an integer optimization model that optimizes the placement of racks of servers within a data center to maximize demand coverage, adhere to space, power and cooling restrictions, and pace resource utilization for future demand. We also define a tractable single-sample online approximation (SSOA) approach to multi-stage stochastic optimization, which approximates unknown parameters with a single realization and re-optimizes decisions dynamically. Theoretical results provide strong performance guarantees of SSOA in the canonical online generalized assignment and online bin packing settings. Computational results using real-world data show that our optimization approach can enhance utilization and reduce power stranding in data centers. Following iterative improvements in collaboration with data center managers, our algorithm has been packaged into a software solution deployed in Microsoft’s data centers worldwide. Deployment data indicate a significant increase in adoption, leading to improved power utilization, multi-million-dollar annual cost savings, and concomitant savings in greenhouse gas emissions. Ultimately, this paper constitutes one of the first large-scale deployments of a decision-making tool in data centers, contributing an interactive decision-making process at the human-machine interface.

Key words: integer optimization, online optimization, sample average approximation, cloud supply chain

1. Introduction

By powering online activity—large-scale analytics, remote conferencing, e-commerce, digital communications, video streaming—the cloud computing industry amounts to hundreds of billions of dollars in market size, with double-digit annual growth projections (Statista 2022). At the core of cloud supply chains, a global network of data centers hosts hardware equipment to power cloud computing services. Data centers play a critical role toward efficient, reliable, and sustainable cloud supply chains, recognized as an emerging area in operations management research (Chen et al. 2023). Specifically, efficiency objectives aim to maintain high data center utilization to serve large volumes of jobs at low cost given limitations in storage space, power resources and cooling

equipment. The reliability objective seeks operational continuity when a device is taken offline. In practice, high utilization may lead to system overloads and service outages, with high financial tolls—millions of dollars for severe outages. Data centers typically add buffers to avoid outages, but these conservative procedures also come with a huge price tag: in 2013, up to 40% of power resources were wasted in US data centers, with a \$3 billion impact ([National Resources Defense Council 2014](#)). Finally, wasted power in data centers contributes to energy usage and greenhouse gas emissions ([International Energy Agency 2022](#)), therefore compounding the goals of enabling high utilization and ensuring reliable service toward sustainable cloud supply chains.

As part of this overarching challenge, an emerging problem is to allocate incoming cloud demand within a data center. Cloud demand materializes as requests for *racks*, which are steel frameworks that host servers, cables, and other computing equipment. Each rack powers billions of queries annually as well as platform as a service, software as a service, and infrastructure as a service functionalities. *Rack placement* decisions are concerned with mounting each rack on a dedicated tile in the data center; these decisions determine the configuration of the data center. Once placed, each rack becomes practically immovable due to labor overhead and financial costs associated with any change in data center configurations. Rack placement decisions need to balance multiple considerations, such as (i) maximizing data center utilization given space, power, and cooling limitations; (ii) ensuring the reliability of cloud computing operations in the event of a power device failure; and (iii) pacing resource utilization to reserve capacity for future demand. In practice, data center managers typically make these decisions based on domain expertise and spreadsheet tools, leading to high mental overload and operating inefficiencies ([Uptime Institute 2014](#)).

In response, this paper provides optimization algorithms and software tools to support data center managers’ rack placement decisions, with the objectives of improving data center efficiency, reliability, and sustainability. From a technical standpoint, rack placement combines the challenges of large-scale combinatorial optimization and online stochastic optimization. At its core, the problem features elements of bin packing to find the smallest possible data center configuration, as well as elements of generalized assignment to allocate racks without exceeding multi-dimensional capacities from space, power, and cooling capacities. However, rack placement departs from canonical resource allocation settings due to combinatorial complexities arising from the layout of data centers, a multi-layer power architecture, reliability requirements, and multi-rack demand requests (see details in Section 3). In addition, racks have to be placed dynamically under demand uncertainty, but placements become practically irreversible thereafter. Therefore, this problem exhibits an online combinatorial optimization structure with irrevocable decisions at each time period.

This paper develops an online rack placement algorithm to optimize large-scale data center configurations with uncertain demand. We formulate an integer optimization model that maximizes

successful placements under capacity constraints and operational requirements. We implement the model in a rolling horizon, with tailored objectives that pace capacity utilization for future demand. Moreover, we propose a single-sample online approximation (SSOA) algorithm that approximates any multi-stage stochastic optimization problem by sampling a single realization of unknown parameters and re-optimizing decisions dynamically. By design, SSOA is much more tractable than multi-sample stochastic programming approaches such as sample average approximation and scenario reduction, at the cost of a simpler representation of uncertainty. We provide theoretical results that show that SSOA yields strong performance guarantees in the canonical online bin packing and online generalized assignment problems. Computational results using real-world data also show its tractability and benefits for the online rack placement problem.

Motivated by the scalability of the optimization formulation and the SSOA algorithm as well as the promising computational results, we have deployed the optimization solution across Microsoft’s fleet of data centers. As with many supply chain problems, rack placement involves complex practical considerations that are hard to elicit in a single optimization model, so it is critical to leverage data center managers’ expertise and empower human decision-making. Accordingly, we have closely collaborated with multiple stakeholders to improve the model and turn it into an effective decision-support tool. Deployment data show a significant increase in adoption over time, leading to improvements in power utilization and multi-million-dollar annual cost savings across Microsoft’s fleet of data centers, along with concomitant reductions in greenhouse gas emissions. Ultimately, this paper constitutes one of the first large-scale deployments of a decision-making tool in data centers, contributing an interactive decision-making process at the human-machine interface.

Specifically, this paper makes the following contributions to the literature:

- *An integer optimization model of rack placement.* We formulate an offline model to optimize the placement of incoming demand requests in the data center. The objective is to maximize demand coverage and minimize operational complexity, given multidimensional resource limitations under regular conditions and in the event of a power device failure. We propose an online rolling-horizon implementation to optimize rack placements for each batch of incoming demand, while ensuring consistency with past placements and reserving resource capacities for future requests.

- *The single-sample online approximation (SSOA) algorithm, with theoretical guarantees in canonical online resource allocation problems.* SSOA provides a tractable approximation of multi-stage stochastic optimization combining a single-sample representation of uncertainty and online re-optimization. In online generalized assignment, we show that SSOA provides a $(1 - \varepsilon_{m,d,T,B})$ -approximation of the perfect-information optimum in expectation, where $\varepsilon_{m,d,T,B}$ scales approximately with the number of supply nodes m (i.e., number of bins) and the dimension d (i.e., number of resources) as $\mathcal{O}(\sqrt{\log(md)})$, with the time horizon T (i.e., number of items) as $\mathcal{O}(\sqrt{\log T})$ and

with resource capacities B as $\mathcal{O}(1/\sqrt{B})$. In particular, this result shows that SSOA is asymptotically optimal if capacities scale with the time horizon as $\Omega(T^\sigma)$ for $\sigma > 0$. We also prove that SSOA achieves sub-linear regret in online bin packing with batched demand, as long as the batches are large enough (e.g., if the batch size grows with the number of items n as $\mathcal{O}(n^\delta)$ for $\delta > 0$). These results motivate an SSOA implementation with batched demand for online rack placement.

- *Evidence of the benefits of the proposed optimization approach.* Based on real-world data on rack demand and the layout of data centers, computational results show the combined benefits of the integer optimization formulation and the SSOA algorithm. Together, they increase utilization by over 5% and reduce power stranding by 50%, as compared with a simpler one-request-at-a-time baseline. Our optimization approach can achieve near-ideal utilization in large-scale data centers, while balancing utilization to ensure reliability in the event of device failures.

- *Realized benefits in production across Microsoft’s data centers.* We have packaged our optimization algorithm into a decision-support software for data center managers. We gathered continual feedback from stakeholder groups and improved the model iteratively through phased deployment. Since its launch in March 2022, the software’s recommendations have been increasingly followed by data center managers, enabling significant improvements in data center configurations. We document reductions in power stranding by 10–30%, or 1–1.5 percentage points as a result, while abiding with operational and reliability requirements. Given the scale of cloud computing, these benefits represent very large efficiency and sustainability gains across the cloud supply chain that translate into multi-million-dollar annual cost savings across Microsoft data centers.

2. Literature Review

Cloud supply chain optimization. Data center operations involve several intertwined optimization problems. At the upstream level, the design of data centers aims to maximize capacity, enable efficient cooling and power consumption, and minimize energy use (Li et al. 2011, Fan et al. 2007, Dayarathna et al. 2016, Zou et al. 2021). Within this area, Arbabian et al. (2021) optimized server procurement for capacity expansion; and Liu et al. (2023) proposed a two-stage stochastic optimization model for capacity expansion under demand uncertainty. A subsequent problem involves allocating incoming demand to data centers (Xu and Li 2013). At the downstream level, the management of cloud infrastructure relies on algorithms to assign jobs to virtual machines (Harchol-Balter 2013, Schroeder et al. 2006, Gardner et al. 2017, Grosf et al. 2022) and virtual machines to servers (Li et al. 2015, Cohen et al. 2019, Gupta and Radovanovic 2020, Perez-Salazar et al. 2022, Buchbinder et al. 2022, Liu and Tang 2022, Muir et al. 2024).

Within this literature, our paper addresses the emerging problem of rack placement, which involves allocating physical servers within a data center. This problem arises at an intermediate

level, after the design of data centers and the allocation of demand across data centers, but prior to the management of jobs and virtual machines. In recent studies, [Zhang et al. \(2021\)](#) proposed a flexible assignment of incoming demand to power devices; and [Mellou et al. \(2023\)](#) developed an online scheduling algorithm to manage power capacities under regular and failover conditions. Our paper contributes a comprehensive optimization approach to efficiently and reliably manage demand and supply within a data center, which captures real-world complexities such as space, power and cooling capacities, regular and failover conditions, and multi-rack demand requests.

Our paper also relates to the deployment of software tools in large-scale data centers. [Radovanović et al. \(2022\)](#) developed a scheduling software to mitigate the carbon footprint of Google’s data centers. [Wu et al. \(2016\)](#) deployed a dynamic power-capping software in Facebook’s data centers. [Lyu et al. \(2023\)](#) introduced a fail-in-place operational model for servers with degraded components in Microsoft’s data centers. Our paper contributes a new solution to support rack placements, which requires a granular representation of cloud demand and data center operations.

Stochastic optimization. Rack placement features a multi-stage integer optimization structure under uncertainty, which could be solved, for example, via stochastic programming ([Birge and Louveaux 2011](#)), approximate dynamic programming ([Powell 2022](#)), and reinforcement learning ([Sutton and Barto 2018](#)). To represent uncertainty, the well-known sample average approximation (SAA) approach approximates probability distributions with a large number of scenarios ([Kleywegt et al. 2002](#)). The SAA method is asymptotically optimal and has shown considerable success, but can still lead to significant computational requirements in practice. The scenario reduction literature seeks instead small-sample approximations of stochastic optimization problems ([Römisch 2009](#), [Bertsimas and Mundru 2022](#), [Zhang et al. 2023](#)). A related theoretical question is to estimate the number of samples required to generate high-quality approximations in the data-driven newsvendor model ([Levi et al. 2015](#), [Cheung and Simchi-Levi 2019](#), [Besbes and Mouchtaki 2023](#)). Yet, even with few scenarios, multi-stage stochastic integer optimization remains challenging. Motivated by tractability objectives, our SSOA algorithm goes one step further by approximating probability distributions with a single sample path at each stage and re-optimizing decisions dynamically.

The SSOA algorithm falls into re-solving heuristics and certainty-equivalent controls in online optimization. These approaches solve a deterministic mathematical program (DMP) at each epoch, typically using the expected value of uncertain parameters ([Bertsekas 2012](#), [Maglaras and Meissner 2006](#), [Secomandi 2008](#), [Wang and Wang 2022](#)). In network revenue management, [Jasin and Kumar \(2012\)](#) and [Bumpensanti and Wang \(2020\)](#) augmented the DMP solution with probabilistic and thresholding rules to achieve bounded regret. Bounded losses have also been obtained with other re-solving heuristics for online resource allocation problems with irrevocable decisions, such as

a budget-ratio policy for the multi-secretary problem (Arlotto and Gurvich 2019), a dynamic Bayesian selection policy in online allocation (Vera and Banerjee 2021), and an empirical DMP with thresholding in a broader class of problems spanning online bin packing and generalized assignment (Banerjee and Freund 2019). Related to our approach, algorithms based on a single sample path have been designed in revenue management (Freund and Zhao 2021) and in the context of prophet inequalities (Azar et al. 2014, Rubinstein et al. 2019, Caramanis et al. 2022).

Our SSOA approach proposes a tractable re-solving heuristic where the problem at each epoch is approximated via a deterministic (mixed-integer) optimization model based on one single sample of uncertainty. This approach provides an easily-implementable and generalizable algorithm in multi-stage stochastic optimization, which does not rely on problem-specific probabilistic or thresholding rules. This paper contributes new theoretical guarantees on the SSOA performance in online bin packing and generalized assignment, and computational results in our rack placement problem.

3. Background: Rack Placement in Microsoft Data Centers

Cloud demand. Demand for Microsoft’s cloud capacity originates from engineering groups (e.g., Azure, Bing, Office, Teams) to host virtual machines, perform computing jobs, and serve their end customers. Within a data center, each demand request materializes in the form of one or several racks of servers, each requiring a certain amount of supporting equipment such as power and cooling. Figure 1 provides empirical distributions of the requirements of demand requests.

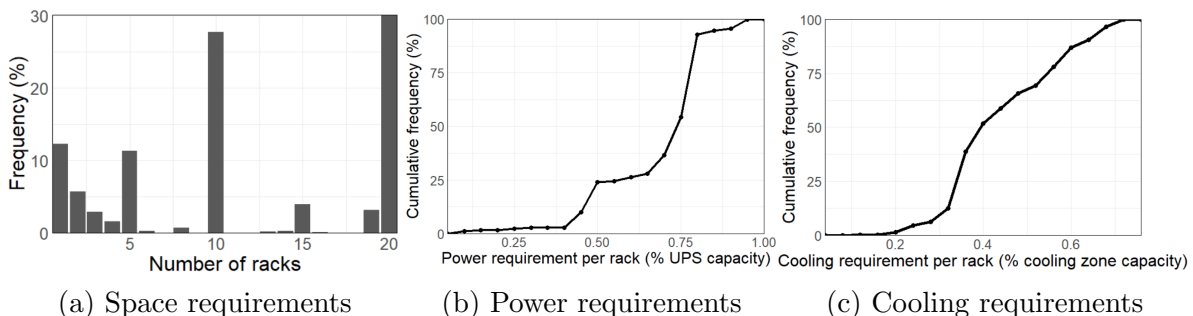


Figure 1 Demand distribution across Microsoft’s data centers.

Each rack must be mounted on a dedicated tile that needs to be powered with appropriate power and cooling equipment. These placements determine the data center configuration. Once placed, racks can hardly be moved to other tiles due to the operational overhead associated with any change in the data center configuration. In our model, we treat rack placement decisions as irrevocable, although decommissions and re-assignments may occur occasionally in practice.

Demand requests arrive sequentially to the data centers. Thus, incoming requests need to be handled without knowledge of future requests. Our model allows batched demand to alleviate the costs of online decision-making.

Data centers. Microsoft operates hundreds of data centers worldwide, each comprising several rooms with thousands of servers (Figure 2a). The main computing equipment is located in server halls, and the primary cooling systems and power generators are stored in adjacent mechanical and electrical yards (Barroso et al. 2019). In this paper, we consider a fixed and exogenous data center architecture, and we focus on the allocation of incoming demand within the data center.

The data center architecture creates three operating bottlenecks:

1. *Physical space.* Each data center has a fixed number of rooms; each room is partitioned into storage rows; each row comprises a set of tiles (computer cabinets); and each tile can fit exactly one rack of servers. All racks from the same demand request must be placed on the same row, due to efficiency considerations (e.g., network latency) and ease of operations.

2. *Power equipment.* Each room is connected to a three-level power hierarchy: Uninterruptible Power Supplies (UPS) devices route power from electrical yards to each room; Power Delivery Units (PDU) devices then route power to the data center floor; and Power Supply Units (PSU) devices distribute power to the tiles. This hierarchy defines a tree-based structure that encodes which PDUs are connected to each UPS, and which PSUs are connected to each PDU (Figure 2b).

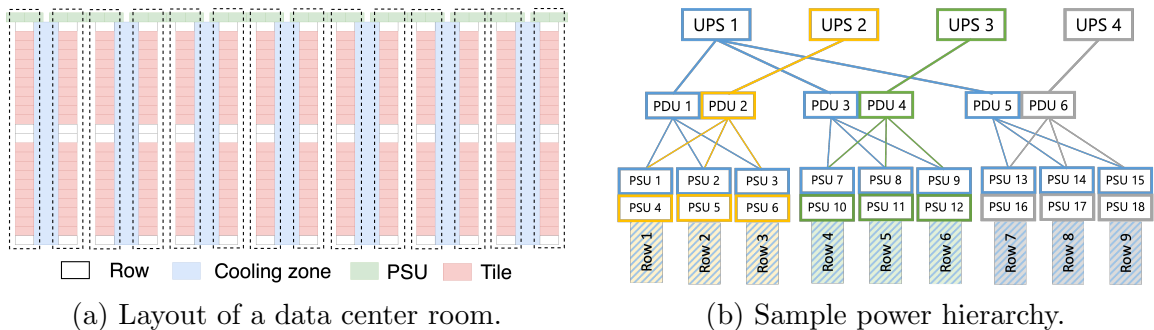


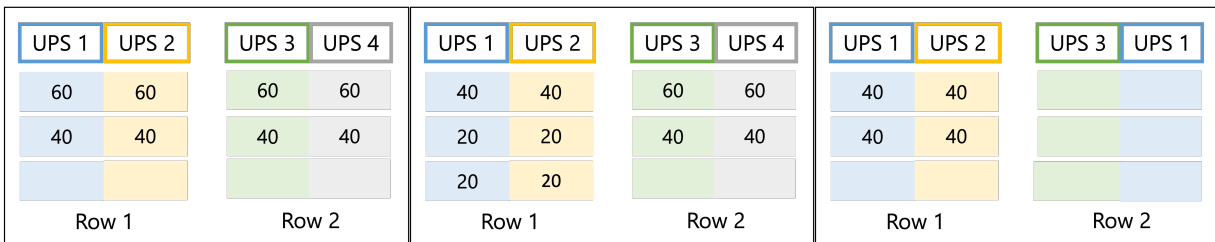
Figure 2 Visualization of the three main operating bottlenecks in data centers: space, power and cooling.

Power device failures represent one of the major sources of data center unreliability. For reliability purposes, data centers are configured with redundant power architectures (Zhang et al. 2021). In Microsoft data centers, redundancy is implemented by powering each tile with two leaf-level PSUs, each connected to different mid-level PDU devices and top-level UPS devices (Figure 2b). When all devices are online, a tile obtains half of its power from each set of devices. Whenever a power device fails or is taken offline, all affected tiles must derive their power from the surviving devices.

Each power device is limited by its regular and failover capacities. The failover capacity is larger than the regular capacity but can only be supplied for a limited amount of time until other devices are taken back online. Thus, rack placements need to comply with multiple capacity restrictions across the power hierarchy (UPS, PDU, and PSU) under both regular and failover conditions.

3. *Cooling equipment*: Each room includes several capacitated cooling zones that host necessary equipment to support the computing hardware. Each tile is connected to one cooling zone.

These bottlenecks can cause inefficiencies and wasted resources. Since power represents the main source of inefficiency, we define a *stranded power* metric as the percentage of power that cannot be used to serve demand requests. Power stranding stems from three sources, illustrated in Figure 3 in simple examples with two rows with three tiles each. Each row is powered by two distinct PSU devices connected to two distinct PDU devices and two distinct UPS devices (for simplicity, we focus in these examples on UPS capacity, which is the main power bottleneck). In all three examples, the two rows have sufficient overall space and power capacity to accommodate the incoming 80-watt request; however, in neither case the incoming request can be added to the configuration.



(a) Power fragmentation.

(b) Resource unavailability.

(c) Failover risk.

Figure 3 Illustration of the sources of power stranding, for a single-rack request with an 80-watt power requirement. Each UPS device has a regular capacity of 120 watts and a failover capacity of 180 watts.

The first source of power stranding is *power fragmentation* (Figure 3a): residual power is spread across devices, leaving no feasible placement for incoming requests (a common challenge in bin packing). In the example, each row has residual capacity of 40 watts and cannot handle the incoming 80-watt request. The second one is *resource unavailability* (Figure 3b): all power devices with residual power are constrained by other resources, such as space or cooling (a common challenge in multi-dimensional generalized assignment). In the example, UPS 1 and UPS 2 have sufficient residual power but are only connected to occupied tiles. The third one is *failover risk* (Figure 3c): a request could be accommodated under regular conditions but no power device has sufficient failover capacity to handle it if another power device fails (a new challenge due to reliability requirements in rack placement). In the example, Row 2 could accommodate the incoming request under regular conditions; however, if UPS 2 were to fail, UPS 1 would need to handle 160 watts in Row 1 and 40 watts in Row 2, in excess of its 180-watt failover capacity. These inefficiencies motivate a new optimization-based approach to support combinatorial rack placement decisions in order to maximize data center utilization while satisfying reliability requirements.

Rack placement in practice. Data center managers are experts in cloud computing who oversee all aspects of data center operations, such as deploying new software and hardware, addressing IT issues, and serving customer requests. In particular, they are in charge of managing demand and supply by determining the data center configuration and monitoring system utilization.

Rack placement decisions are traditionally based on human expertise. For each demand request, data center managers analyze various placements using spreadsheet tools. Any tentative placement is validated by a feasibility-oriented software that checks for resource availability. Due to cloud computing growth, rack placement decisions have become increasingly complex with many interdependent and conflicting objectives, leading to high mental loads and operational inefficiencies.

This paper proposes a new software tool to support rack placement. Due to the complexity of rack placement, our goal is not to deploy an automated decision-making system. Instead, we package our algorithm into a decision-support software that provides rack placement suggestions, so that data center managers retain decision-making authority to accept or reject these recommendations. By facilitating human-machine interactions, this collaborative decision-making process combines the strengths of the optimization methodology and of data center managers' expertise.

4. The Rack Placement Problem

4.1. Mathematical Notation

Demand. Let \mathcal{D} denote the set of requests. Each request $d \in \mathcal{D}$ involves n_d racks of servers, each requiring ρ_d units of power and γ_d units of cooling. A request is satisfied if *all* racks are placed.

Space. The physical layout of the data center is characterized by a set of rows \mathcal{R} partitioned into a set of rooms \mathcal{M} . The room of row $r \in \mathcal{R}$ is denoted by $rm(r) \in \mathcal{M}$.

Cooling. Let \mathcal{C} denote the set of cooling zones. Each cooling zone $c \in \mathcal{C}$ has capacity C_c . Each row $r \in \mathcal{R}$ is connected to one cooling zone, denoted by $cz(r) \in \mathcal{C}$.

Power. Let \mathcal{P} denote the set of power devices, partitioned into $\mathcal{P} = \mathcal{P}^{PSU} \cup \mathcal{P}^{PDU} \cup \mathcal{P}^{UPS}$ (Figure 2b). For UPS $p \in \mathcal{P}^{UPS}$, we denote by $\mathcal{L}_p \subset \mathcal{P}$ the subset of power devices connected to it, i.e., \mathcal{L}_p includes p itself, all PDUs connected to p , and all PSUs connected to a PDU in \mathcal{L}_p . Each device $p \in \mathcal{P}$ has capacity P_p under regular conditions and $F_p > P_p$ under failover conditions. In the rack placement problem, we protect against any one-off UPS failure (as in Zhang et al. 2021). This approach trades off efficiency and reliability by protecting against the most impactful failures (protecting against top-level UPS failures also protects against lower-level PDU and PSU failures) but protecting against one failure at a time (in practice, simultaneous failures are extremely rare).

Tile groups. The rack placement problem assigns each rack to a hardware tile, which determines the cooling zone and two redundant PSU devices. Rather than optimizing rack-tile assignments and linking these decisions to space, cooling and power utilization, we optimize the number of

racks from each request that are assigned to *tile groups*, stored in a set \mathcal{G} . This approach simplifies the formulation and reduces model symmetry. Each tile group $g \in \mathcal{G}$ is characterized as the set of indiscernible tiles located in the same row and connected to the same pair of PSU devices. Let $row(g) \in \mathcal{R}$ denote the row of tile group $g \in \mathcal{G}$. Let $\mathcal{G}_p \subset \mathcal{G}$ denote the set of tile groups connected to power device $p \in \mathcal{P}$; this definition captures the connections between hardware tiles and PSU devices (for $p \in \mathcal{P}^{PSU}$), as well as the indirect connections within the three-level power hierarchy (for $p \in \mathcal{P}^{PDU} \cup \mathcal{P}^{UPS}$). Finally, we denote by s_g the number of tiles in group $g \in \mathcal{G}$.

Table 1 summarizes the notation described above.

Component	Notation	Description
Set	\mathcal{R}	Rows
	\mathcal{M}	Rooms
	\mathcal{P}	Power devices
	\mathcal{C}	Cooling zones
	\mathcal{G}	Tile groups with same row and PSU devices
	\mathcal{D}	Demand requests to be placed
	\mathcal{P}^{UPS}	UPS power devices at the top level
	\mathcal{P}^{PDU}	PDU power devices at the middle level
	\mathcal{P}^{PSU}	PSU power devices at the leaf level
		\mathcal{L}_p
	\mathcal{G}_p	Tile groups in \mathcal{G} connected to power device $p \in \mathcal{P}$
Index	$rm(r)$	Room in \mathcal{M} of row $r \in \mathcal{R}$
	$cz(r)$	Cooling zone in \mathcal{C} of row $r \in \mathcal{R}$
	$row(g)$	Row in \mathcal{R} of tile group $g \in \mathcal{G}$
Parameter	n_d	Number of racks in request $d \in \mathcal{D}$
	ρ_d	Power requirement per rack of request $d \in \mathcal{D}$ in watts
	γ_d	Cooling requirement per rack of request $d \in \mathcal{D}$ in cubic feet per minute
	s_g	Number of tiles in tile group $g \in \mathcal{G}$
	P_p	Regular capacity of power device $p \in \mathcal{P}$ in watts
	F_p	Failover capacity of power device $p \in \mathcal{P}$ in watts
	C_c	Capacity of cooling zone $c \in \mathcal{C}$ in cubic feet per minute
	μ	Reward for placing one request
	λ_m	Penalty for placing a request in room $m \in \mathcal{M}$
	τ	Penalty to assign any request to a tile group

Table 1 Notation for the rack placement models.

4.2. Integer Optimization Formulation for Offline Rack Placement

The primary decision variables \mathbf{u} define the assignment of racks to three-dimensional tile groups, and auxiliary variables track the impact on utilization and operational complexity:

$$u_{dg} : \text{number of racks from request } d \in \mathcal{D} \text{ assigned to tile group } g \in \mathcal{G}.$$

$$w_{dm} = \begin{cases} 1 & \text{if request } d \in \mathcal{D} \text{ is placed in room } m \in \mathcal{M}, \\ 0 & \text{otherwise.} \end{cases}$$

$$x_{dg} = \begin{cases} 1 & \text{if tile group } g \in \mathcal{G} \text{ is used to serve request } d \in \mathcal{D}, \\ 0 & \text{otherwise.} \end{cases}$$

$$y_{dr} = \begin{cases} 1 & \text{if request } d \in \mathcal{D} \text{ is assigned to row } r \in \mathcal{R}, \\ 0 & \text{otherwise.} \end{cases}$$

The offline rack placement problem is formulated as follows:

$$\max \quad \mu \sum_{d \in \mathcal{D}} \sum_{r \in \mathcal{R}} y_{dr} - \sum_{d \in \mathcal{D}} \sum_{m \in \mathcal{M}} \lambda_m w_{dm} - \tau \sum_{d \in \mathcal{D}} \sum_{g \in \mathcal{G}} x_{dg} \quad (1)$$

$$\text{s.t. } u_{dg} \leq \min \{n_d, s_g\} y_{d, \text{row}(g)} \quad \forall d \in \mathcal{D}, \forall g \in \mathcal{G} \quad (2)$$

$$u_{dg} \leq \min \{n_d, s_g\} x_{dg} \quad \forall d \in \mathcal{D}, \forall g \in \mathcal{G} \quad (3)$$

$$y_{dr} \leq w_{d, \text{rm}(r)} \quad \forall d \in \mathcal{D}, \forall r \in \mathcal{R} \quad (4)$$

$$\sum_{r \in \mathcal{R}} y_{dr} \leq 1 \quad \forall d \in \mathcal{D} \quad (5)$$

$$\sum_{g \in \mathcal{G}} u_{dg} = n_d \sum_{r \in \mathcal{R}} y_{dr} \quad \forall d \in \mathcal{D} \quad (6)$$

$$\sum_{d \in \mathcal{D}} u_{dg} \leq s_g \quad \forall g \in \mathcal{G} \quad (7)$$

$$\sum_{d \in \mathcal{D}} \sum_{\substack{g \in \mathcal{G}: \\ \text{cz}(\text{row}(g))=c}} \gamma_d u_{dg} \leq C_c \quad \forall c \in \mathcal{C} \quad (8)$$

$$\sum_{d \in \mathcal{D}} \sum_{g \in \mathcal{G}_p} \frac{\rho_d}{2} u_{dg} \leq P_p \quad \forall p \in \mathcal{P} \quad (9)$$

$$\sum_{d \in \mathcal{D}} \left(\sum_{g \in \mathcal{G}_p} \frac{\rho_d}{2} u_{dg} + \sum_{g \in \mathcal{G}_p \cap \mathcal{G}_t} \frac{\rho_d}{2} u_{dg} \right) \leq F_p \quad \forall t \in \mathcal{P}^{UPS}, \forall p \in \mathcal{P} \setminus \mathcal{L}_t \quad (10)$$

$$\mathbf{u} \text{ integer, } \mathbf{w}, \mathbf{x}, \mathbf{y} \text{ binary.} \quad (11)$$

Equation (1) maximizes utilization (number of successful placements) while minimizing operational complexity (number of rooms opened and number of active tile groups). The parameters μ , λ_m and τ trade off these objectives. We model λ_m as a heterogeneous penalty to discourage placing incoming requests in emptier rooms: a room $m \in \mathcal{M}$ with a larger proportion of occupied tiles is associated with a smaller λ_m . Constraints (2)–(4) define the utilization of tile groups, rows and rooms. Constraints (5) state that all racks from a request must be assigned to the same row. Constraints (6) convey that a request is placed if all of its racks are assigned to a tile group. The next constraints apply the space capacities (Constraints (7)), cooling capacities (Constraints (8)) and power capacities under regular operations (Constraints (9)). The factor $\rho_d/2$ reflects that the power requirements of each rack are shared by the two connected PSU devices and by the two sets of connected PDU devices and UPS devices. Finally, Constraints (10) ensure that the increased power load abides by the failover capacity of device $p \in \mathcal{P}$ under any one-off UPS device failure.

The left-hand side reflects that, whenever one UPS device $t \in \mathcal{P}^{UPS}$ is taken down, the power requirements of all corresponding tile groups $g \in \mathcal{G}_t$ must be handled by the surviving devices.

4.3. Rolling Horizon Implementation with Batched Demand

We apply the rack placement model in a rolling horizon with batched demand. At each decision epoch, inputs characterize active requests (which were placed earlier) and the batch of incoming requests (which need to be placed immediately). To avoid myopic decision-making, we introduce additional objectives that pace residual resources to reserve capacity for future demand requests.

Batched demand. The set \mathcal{D} collects the batch of incoming requests. Let \mathcal{A} be the set of active requests that have already been placed and therefore cannot be moved. Each request $d \in \mathcal{A}$ has a_{dg} racks already assigned to tiles from group $g \in \mathcal{G}$, analogous to the decision variables u_{dg} . We denote by $\mathcal{G}' \subseteq \mathcal{G}$ the subset of tile groups that still have available tiles. Similarly, \mathcal{R}' , \mathcal{M}' , \mathcal{C}' , and \mathcal{P}' respectively store the rows, rooms, cooling zones, and power devices with available capacity:

$$\begin{aligned} \mathcal{G}' &= \left\{ g \in \mathcal{G} : s_g - \sum_{d \in \mathcal{A}} a_{dg} > 0 \right\} \\ \mathcal{R}' &= \{ r \in \mathcal{R} : \exists g \in \mathcal{G}', \text{row}(g) = r \} & \mathcal{M}' &= \{ m \in \mathcal{M} : \exists r \in \mathcal{R}', \text{rm}(r) = m \} \\ \mathcal{C}' &= \{ c \in \mathcal{C} : \exists r \in \mathcal{R}', \text{cz}(r) = c \} & \mathcal{P}' &= \{ p \in \mathcal{P} : \mathcal{G}_p \cap \mathcal{G}' \neq \emptyset \}. \end{aligned}$$

We replace the capacity constraints in Equations (7)–(10) with the following constraints to account for the space, cooling and power utilization from active requests in the set \mathcal{A} :

$$\sum_{d \in \mathcal{D}} u_{dg} \leq s_g - \sum_{d \in \mathcal{A}} a_{dg} \quad \forall g \in \mathcal{G}' \quad (12)$$

$$\sum_{d \in \mathcal{D}} \sum_{\substack{g \in \mathcal{G}' : \\ \text{cz}(\text{row}(g)) = c}} \gamma_d u_{dg} \leq C_c - \sum_{d \in \mathcal{A}} \sum_{\substack{g \in \mathcal{G}' : \\ \text{cz}(\text{row}(g)) = c}} \gamma_d a_{dg} \quad \forall c \in \mathcal{C}' \quad (13)$$

$$\sum_{d \in \mathcal{D}} \sum_{g \in \mathcal{G}_p \cap \mathcal{G}'} \frac{\rho_d}{2} u_{dg} \leq P_p - \sum_{d \in \mathcal{A}} \sum_{g \in \mathcal{G}_p} \frac{\rho_d}{2} a_{dg} \quad \forall p \in \mathcal{P}' \quad (14)$$

$$\sum_{d \in \mathcal{D}} \left(\sum_{g \in \mathcal{G}_p \cap \mathcal{G}'} \frac{\rho_d}{2} u_{dg} + \sum_{g \in \mathcal{G}_p \cap \mathcal{G}_t \cap \mathcal{G}'} \frac{\rho_d}{2} u_{dg} \right) \leq F_p - \sum_{d \in \mathcal{A}} \left(\sum_{g \in \mathcal{G}_p} \frac{\rho_d}{2} a_{dg} + \sum_{g \in \mathcal{G}_p \cap \mathcal{G}_t} \frac{\rho_d}{2} a_{dg} \right) \quad \forall t \in \mathcal{P}^{UPS}, \forall p \in \mathcal{P}' \setminus \mathcal{L}_t \quad (15)$$

Online objectives. In the online implementation of the model, we add online objectives to pace the utilization of space and power resources in the data center for future demand. We provide examples and intuition underlying these objectives in [EC.1.1](#).

– *Row minimization.* This objective aims to consolidate requests amongst fewer rows in order to reserve space for large future requests. We introduce a new variable $z_r \in \{0, 1\}$ indicating whether row $r \in \mathcal{R}'$ is utilized in the incoming batch \mathcal{D} . We add a term $-\sum_{r \in \mathcal{R}'} \theta_r z_r$ to the objective

function to penalize placements on emptier rows, where θ_r is larger for rows $r \in \mathcal{R}'$ with fewer placed racks. We add the following constraints to ensure the consistency between variables, by enforcing that $z_r = 1$ whenever a demand request is placed in row $r \in \mathcal{R}'$:

$$u_{dg} \leq \min \left\{ n_d, s_g - \sum_{d \in \mathcal{A}} a_{dg} \right\} z_{row(g)}, \quad \forall d \in \mathcal{D}, \forall g \in \mathcal{G}'. \quad (16)$$

– *Power surplus and power balance.* These objectives encourage balanced power loads to reduce power stranding. Let \mathcal{P}_m^{UPS} store the top-level power devices in room $m \in \mathcal{M}'$. The power surplus objective minimizes the surplus load $\Phi \in \mathbb{R}_+$ for any pair of top-level UPS devices, defined as the difference from a perfectly balanced load. This is captured by the following constraints:

$$\Phi \geq \sum_{g \in \mathcal{G}_p \cap \mathcal{G}_q \cap \mathcal{G}'} \sum_{d \in \mathcal{D}} \rho_d u_{dg} + \sum_{g \in \mathcal{G}_p \cap \mathcal{G}_q} \sum_{d \in \mathcal{A}} \rho_d a_{dg} - \frac{1}{\binom{|\mathcal{P}_m^{UPS}|}{2}} \sum_{t \in \mathcal{P}_m^{UPS}} P_t, \quad \forall m \in \mathcal{M}', \forall p, q \in \mathcal{P}_m^{UPS}. \quad (17)$$

The power balance objective minimizes the largest power load difference across all pairs of top-level UPS devices. This is written as $\Psi - \Omega$, where $\Psi, \Omega \in \mathbb{R}_+$ are defined as follows:

$$\Psi \geq \sum_{g \in \mathcal{G}_p \cap \mathcal{G}_q \cap \mathcal{G}'} \sum_{d \in \mathcal{D}} \rho_d u_{dg} + \sum_{g \in \mathcal{G}_p \cap \mathcal{G}_q} \sum_{d \in \mathcal{A}} \rho_d a_{dg}, \quad \forall m \in \mathcal{M}', \forall p, q \in \mathcal{P}_m^{UPS}, \quad (18)$$

$$\Omega \leq \sum_{g \in \mathcal{G}_p \cap \mathcal{G}_q \cap \mathcal{G}'} \sum_{d \in \mathcal{D}} \rho_d u_{dg} + \sum_{g \in \mathcal{G}_p \cap \mathcal{G}_q} \sum_{d \in \mathcal{A}} \rho_d a_{dg}, \quad \forall m \in \mathcal{M}', \forall p, q \in \mathcal{P}_m^{UPS}. \quad (19)$$

Online formulation. Our proposed formulation for the online rack placement problem is given in Equations (20)–(26). Equation (20) captures the aforementioned online objectives to pace resource utilization over time. Constraints (12)–(15) adjust resource capacities to account for active requests. Constraints (16)–(19) define the new objectives of row minimization, power surplus, and power balance. Constraints (21)–(26) are analogous to Constraints (2)–(11):

$$\max \sum_{d \in \mathcal{D}} \left(\mu \sum_{r \in \mathcal{R}'} y_{dr} - \sum_{m \in \mathcal{M}'} \lambda_m w_{dm} - \tau \sum_{g \in \mathcal{G}'} x_{dg} \right) - \sum_{r \in \mathcal{R}'} \theta_r z_r - \alpha \Phi - \beta (\Psi - \Omega) \quad (20)$$

s.t. Constraints (12)–(19)

$$u_{dg} \leq \min \left\{ n_d, s_g - \sum_{f \in \mathcal{A}} a_{fg} \right\} y_{d, row(g)} \quad \forall d \in \mathcal{D}, \forall g \in \mathcal{G}' \quad (21)$$

$$u_{dg} \leq \min \left\{ n_d, s_g - \sum_{f \in \mathcal{A}} a_{fg} \right\} x_{dg} \quad \forall d \in \mathcal{D}, \forall g \in \mathcal{G}' \quad (22)$$

$$y_{dr} \leq w_{d, rm(r)} \quad \forall d \in \mathcal{D}, \forall r \in \mathcal{R}' \quad (23)$$

$$\sum_{r \in \mathcal{R}'} y_{dr} \leq 1 \quad \forall d \in \mathcal{D} \quad (24)$$

$$\sum_{g \in \mathcal{G}'} u_{dg} = n_d \sum_{r \in \mathcal{R}'} y_{dr} \quad \forall d \in \mathcal{D} \quad (25)$$

$$\mathbf{u} \text{ integer, } \mathbf{w}, \mathbf{x}, \mathbf{y}, \mathbf{z} \text{ binary, } \Phi, \Psi, \Omega \geq 0 \quad (26)$$

5. Single-Sample Online Approximation (SSOA)

The SSOA algorithm for multi-stage stochastic optimization is motivated by the joint needs to account for future uncertainty and to retain tractability at each decision epoch. Multi-sample methods such as sample average approximation (SAA) or even scenario reduction can lead to large scenario trees, which can hinder scalability in complex combinatorial optimization problems such as rack placement. Instead, SSOA provides an easily-implementable and generalizable algorithm that (i) represents uncertainty by a *single* sample path, and (ii) re-optimizes decisions dynamically in a rolling horizon (Section 5.1). Despite its simplicity, SSOA provides strong performance guarantees in canonical online resource allocation problems (Section 5.2). We leverage these theoretical results to guide the application of SSOA for online rack placement (Section 5.3).

5.1. SSOA Algorithm

Consider a generic multi-stage stochastic optimization problem with T time periods. At each period $t = 1, \dots, T$, a decision-maker chooses an action x^t within a feasible region \mathcal{X}^t that reflects period-specific constraints. We characterize uncertainty via random variables V^1, \dots, V^T , which follow a known distribution μ . The objective is to minimize an expected cost function of the actions and the uncertainty; the cost function can also capture linking constraints across time periods:

$$\min \mathbb{E} [\text{cost}(x^1, \dots, x^T; V^1, \dots, V^T)]. \quad (27)$$

The SSOA algorithm relies on an online implementation of a deterministic model to optimize decisions dynamically (Algorithm 1). The deterministic model approximates the distribution μ with a *single* sample path realization at each decision epoch. Note that this single sample captures the uncertainty from distribution μ , as opposed to solely relying on its expected value. Specifically, at each time period $t = 1, \dots, T$, the realization V^t is revealed and a sample of future realizations $\tilde{V}_{t+1}^t, \dots, \tilde{V}_T^t$ is obtained from distribution μ . The decision-maker optimizes $x^t \in \mathcal{X}^t, \dots, x^T \in \mathcal{X}^T$ based on past realizations V^1, \dots, V^t and the sample path $\tilde{V}_{t+1}^t, \dots, \tilde{V}_T^t$. Whereas the reliance on a single sample obviously simplifies the representation of uncertainty, the SSOA algorithm attempts to mitigate errors by allowing dynamic re-optimization. Specifically, only the decision x^t is implemented at time t (we denote it by \bar{x}^t); all remaining decisions x^{t+1}, \dots, x^T are discarded (we denote them by $\tilde{x}^{t+1}, \dots, \tilde{x}^T$) and subject to re-optimization at subsequent decision epochs.

Note that the time discretization and the random variables V^1, \dots, V^T define the extent of batching in the SSOA algorithm. At one extreme, SSOA captures offline optimization with $T = 1$, when V^1 encompasses the full uncertainty. At the other extreme, it captures one-at-a-time decision-making when each random variable V^t corresponds to uncertainty regarding a single item. In-between, the SSOA algorithm reflects a batched optimization approach, where uncertainty is aggregated into T batches and V^1, \dots, V^T represents the uncertainty within each batch.

Algorithm 1 Single-Sample Online Approximation (SSOA) algorithm.

for $t = 1, \dots, T$ **do**

Observe data V^t .

Sample future realizations $\tilde{V}_{t+1}^t, \dots, \tilde{V}_T^t$ independently from distribution μ .

Given implemented decisions $(\bar{x}^1, \dots, \bar{x}^{t-1})$, find an optimal solution $(\bar{x}^t, \bar{x}^{t+1}, \dots, \bar{x}^T)$ for

$$\min_{x^t \in \mathcal{X}^t, \dots, x^T \in \mathcal{X}^T} \text{cost}\left(\bar{x}^1, \dots, \bar{x}^{t-1}, x^t, x^{t+1}, \dots, x^T; V^1, \dots, V^t, \tilde{V}_{t+1}^t, \dots, \tilde{V}_T^t\right).$$

Implement decision \bar{x}^t .

end for

In summary, the SSOA algorithm approximates Equation (27) by combining a single-sample approximation of the uncertainty and online re-optimization in a rolling horizon implementation. This approach can be viewed as a lightweight version of SAA to account for future realizations while retaining computational tractability at each decision point by avoiding large decision trees. As we shall see, it can still provide strong approximations of the perfect-information optimum.

5.2. Theoretical Results: SSOA Approximation Guarantees

We consider two canonical online resource allocation problems: the online generalized assignment problem and the online bin packing problem. Both problems capture some of the core dynamics of online rack placement. In both cases, we show that the SSOA algorithm achieves a strong approximation of the expected offline optimum, defined as the expected cost that can be achieved under perfect information. Throughout this section, we refer to the perfect-information optimum as OPT and its expected value as $\mathbb{E}(\text{OPT})$; and we compare the SSOA solution to $\mathbb{E}(\text{OPT})$.

Generalized assignment problem. This problem optimizes item-bin assignments under multiple resource capacity constraints (Srinivasan and Thompson 1973). It reflects the core rack placement objective of maximizing utilization given the multiple operating bottlenecks. In this analogy, items correspond to racks or demand requests, bins correspond to rooms or storage rows, and resources correspond to space, power devices, and cooling equipment. For simplicity, we ignore demand batching to focus on the role of demand and resource capacities in SSOA performance.

DEFINITION 1 (STOCHASTIC MULTI-DIMENSIONAL GENERALIZED ASSIGNMENT). Items arrive one at a time, indexed by $t = 1, \dots, T$. Each item can be assigned to one of m bins, indexed by $i = 1, \dots, m$. The problem features d resources, and each bin has capacity b_{ij} for resource $j = 1, \dots, d$. The assignment of item t in bin i comes with an unknown value $C_i^t \geq 0$ and consumes an unknown amount $A_{ij}^t \geq 0$ of resource $j = 1, \dots, d$. Both of these quantities are only revealed when the item arrives, and remain unknown for future items. We define binary variables x_i^t indicating whether

item t is placed in bin i . For item t , we define the assignment vector $x^t = (x_1^t, \dots, x_m^t)$, the value vector $C^t = (C_1^t, \dots, C_m^t)$, and the resource requirements matrix $A^t = (A_{ij}^t)_{ij}$. The tuples (C^t, A^t) are drawn independently from a joint distribution μ . The problem maximizes the assignment value subject to resource availability constraints. The reward function is given by:

$$\text{reward}(x^1, \dots, x^T; C^1, \dots, C^T, A^1, \dots, A^T) = \begin{cases} \sum_{t=1}^T \sum_{i=1}^m C_i^t x_i^t & \text{if } \sum_{t=1}^T A_{ij}^t x_i^t \leq b_{ij}, \forall i = 1, \dots, m, \\ & \forall j = 1, \dots, d \\ & \text{and } \sum_{i=1}^m x_i^t \leq 1, \forall t = 1, \dots, T, \\ -\infty & \text{otherwise.} \end{cases}$$

The offline optimum can then be derived from the following integer optimization formulation:

$$\max \sum_{t=1}^T \sum_{i=1}^m C_i^t x_i^t \quad (28)$$

$$\text{s.t. } \sum_{t=1}^T A_{ij}^t x_i^t \leq b_{ij}, \quad \forall i = 1, \dots, m, j = 1, \dots, d \quad (29)$$

$$\sum_{i=1}^m x_i^t \leq 1, \quad \forall t = 1, \dots, T \quad (30)$$

$$\mathbf{x} \text{ binary} \quad (31)$$

Theorem 1 shows that the SSOA algorithm yields a $(1 - \varepsilon_{m,d,T,B})$ -approximation of the expected offline optimum for the multi-dimensional generalized assignment problem (see Algorithm 3 in EC.2 for the instantiation of SSOA to this problem). Specifically, $\varepsilon_{m,d,T,B}$ scales approximately as $\mathcal{O}\left(\sqrt{\frac{\log(mdT)}{B}}\right)$, where m is the number of supply bins, d is the dimension (i.e., number of resources per bin), T is the time horizon (i.e., number of items), and B is the tightest resource capacity (normalized to resource requirements). This result shows a weak dependency in $\mathcal{O}(\sqrt{\log(mdT)})$ with the problem's dimensionality and the time horizon. Moreover, the approximation improves as resource capacities become larger relative to resource requirements, because the larger the capacity, the less constraining initial assignments are for future demand realizations. In fact, if capacities scale as $B = \Omega(T^\sigma)$ for $\sigma > 0$, then the SSOA algorithm becomes asymptotically optimal.

Theorem 1 *The SSOA algorithm returns a feasible solution to the stochastic multi-dimensional generalized assignment problem. Let $\varepsilon \in (0, 0.001]$ be such that $b_{ij} \geq \Omega\left(\log\left(\frac{2mdT}{\varepsilon}\right) \cdot \frac{\log^3(1/\varepsilon)}{\varepsilon^2}\right) A_{ij}^t$ for all $i = 1, \dots, m, j = 1, \dots, d$ and $t = 1, \dots, T$ and for every resource matrix A in the support of μ . Then, the SSOA algorithm returns a solution with expected value at least $(1 - \varepsilon) \cdot \mathbb{E}(\text{OPT})$.*

The proof (in the electronic companion EC.2) follows by (i) deriving the scaling of the expected offline optimum with the time horizon and resource capacities (Lemma EC.1), (ii) showing that the

algorithm uses approximately a fraction t/T of the budget after t periods with high probability and in expectation (Lemmas EC.2 and EC.3) and (iii) showing that each period contributes a reward of approximately $1/T \cdot \mathbb{E}(\text{OPT})$ (Lemma EC.4). A key difficulty lies in the dependence between random variables; for instance, the incremental resource utilization at period t depends on the decision at time t , which itself depends on the utilization in periods $1, \dots, t-1$. This prevents the use of traditional concentration inequalities, so we prove a new concentration inequality for affine stochastic processes that may be of independent interest (Theorem 5 in EC.2.2).

Bin packing problem. This problem optimizes the assignment of heterogeneous jobs to the smallest possible number of homogeneous (unit-sized) bins (Lodi et al. 2002). It captures the core objective of seeking a compact data center configuration under uncertainty regarding future demand requests. In this view, jobs correspond to racks or demand requests, and bins represent rooms or rows. To study the impact of demand batching, we consider a batched bin packing problem in which demand arrives in T batches of q jobs (Gutin et al. 2005).

DEFINITION 2 (STOCHASTIC BATCHED BIN PACKING). Jobs arrive at times $t = 1, \dots, T$ in batches of size q (with $n = Tq$ jobs overall). Each job must be placed in one of m unit-sized bins. The random vector $V^t \in [0, 1]^q$ characterizes the size of the q jobs arriving at time $t = 1, \dots, T$, and is drawn i.i.d. from distribution μ . This vector is only known upon the arrival of the batch. The objective is to minimize the number of opened bins. Binary variables x_{ji}^t indicate whether, at time $t = 1, \dots, T$, job $j = 1, \dots, q$ is placed in bin $i = 1, \dots, m$; and binary variables y_i track whether bin $i = 1, \dots, m$ is open. For convenience, we denote the assignment matrix by $x^t = (x_{ji}^t)_{ji} \in \{0, 1\}^{q \times m}$ and the size vector by $V^t = (V_1^t, \dots, V_q^t)$. The cost function is given by

$$\text{cost}(x^1, \dots, x^T; V^1, \dots, V^T) = \begin{cases} \min \sum_{i=1}^m y_i & \text{s.t. } \sum_{t=1}^T \sum_{j=1}^q V_j^t x_{ji}^t \leq y_i, \forall i = 1, \dots, m, \\ & \sum_{i=1}^m x_{ji}^t = 1, \forall t = 1, \dots, T, \forall j = 1, \dots, q, \\ & \mathbf{y} \text{ binary} \\ & \text{if this problem admits a feasible solution;} \\ +\infty & \text{otherwise.} \end{cases}$$

The offline optimum can be derived from the following integer optimization formulation:

$$\min \sum_{i=1}^m y_i \tag{32}$$

$$\text{s.t. } \sum_{t=1}^T \sum_{j=1}^q V_j^t x_{ji}^t \leq y_i, \quad \forall i = 1, \dots, m \tag{33}$$

$$\sum_{i=1}^m x_{ji}^t = 1, \quad \forall t = 1, \dots, T, \forall j = 1, \dots, q \tag{34}$$

$$\mathbf{x}, \mathbf{y} \text{ binary} \tag{35}$$

We study a slight variant of the SSOA algorithm in which all uncertainties are sampled at the beginning of the horizon—as opposed to being re-sampled in each period (see Algorithm 4 in EC.3). This change simplifies the proofs without impacting the overall methodology.

Theorem 2 shows that the SSOA algorithm yields a $\mathcal{O}\left(\frac{n \log^{3/4} q}{\sqrt{q}}\right)$ loss for the bin packing problem, as long as the batches are large enough. Notably, if $q = \mathcal{O}(n^\delta)$ for $\delta > 0$, this result provides a sublinear regret for the online bin packing problem. Compared to the generalized assignment setting, this result does not depend on the size of the jobs but depends on the number of jobs in each batch. The proof (in EC.3) leverages the monotone matching theorem from Rhee and Talagrand (1993a) to bound the cost difference between the number of bins opened when the decision at time $t = 1, \dots, T$ is based on the true job sizes V^t versus the sampled job sizes \tilde{V}^t .

Theorem 2 *The SSOA algorithm returns a feasible solution to the stochastic bin packing problem. Assume that $\sqrt{q}(\log^{3/4} q) e^{c \cdot \log^{3/2} q} \geq n$, for a sufficiently small constant c . Then, the SSOA algorithm opens in expectation $\mathbb{E}(\text{OPT}) + \mathcal{O}\left(\frac{n \log^{3/4} q}{\sqrt{q}}\right)$ bins.*

Discussion. These results provide theoretical guarantees on the performance of the SSOA algorithm. In online generalized assignment, Theorem 1 yields a $(1 - \varepsilon)$ -approximation, where ε grows logarithmically with the dimension and the time horizon but decreases with the slack in capacities; in online bin packing, Theorem 2 yields a sub-linear regret as long as batches are large enough. These results echo prior literature. In online generalized assignment, Gupta and Molinaro (2016) designed an algorithm with similar guarantees that does not require distributional knowledge. In online bin packing, Rhee and Talagrand (1993a,b) designed an algorithm with a $\sqrt{n \log^{3/4} n}$ loss that also does not require distributional knowledge and that does not depend on the batch size. Our results provide slightly weaker guarantees. However, rather than involving highly specialized algorithms, our results rely on an easily-implementable and generalizable algorithm for multi-stage stochastic optimization that is agnostic to the problem’s structure, combining a single-sample approximation of uncertainty and online re-optimization in a rolling horizon.

These performance guarantees may be surprising given that the SSOA algorithm uses a single sample path. In fact, this sample path plays a critical role in managing resources for future demand. In contrast, a myopic decision-making approach can lead to arbitrarily poor performance. To see this, consider the generalized assignment problem with one bin, T items of size 1, and one resource in quantity $b_{11} = \sqrt{T}$. Assume that item values are equal to 1 with probability $1/\sqrt{T}$ and to a small value $\delta > 0$ with probability $1 - 1/\sqrt{T}$. Since there are on average \sqrt{T} items of value 1, it can be shown that $\mathbb{E}(\text{OPT}) \approx \sqrt{T}$. Per Theorem 1, the SSOA algorithm achieves a value close to the \sqrt{T} optimum for large enough T . However, a myopic decision-making rule would always assign items to the bin until all \sqrt{T} resources have been consumed, leading to an expected value

of $\sqrt{T} \left(1 \cdot \frac{1}{\sqrt{T}} + \delta \cdot \left(1 - \frac{1}{\sqrt{T}} \right) \right) = \delta\sqrt{T} + 1 - \delta \approx \delta\sqrt{T}$. Therefore, a myopic approach achieves a fraction δ of the optimal value, which can be made arbitrarily small.

5.3. SSOA Algorithm for the Online Rack Placement Problem

Online rack placement departs from canonical resource allocation problems, due notably to coupled capacity constraints (e.g., room/row capacities, multi-layer power hierarchy), coupled demand constraints (e.g., multi-rack requests), redundancy constraints, and multiple objectives. Still, Theorems 1 and 2 provide theoretical motivation to leverage the SSOA algorithm in our online rack placement problem. In fact, Theorem 1 underscores the role of capacity buffers, motivating our online objectives to maximize spare capacity for future demand requests; and Theorem 2 underscores the role of batching, motivating our batched optimization approach.

Algorithm 2 details the application of SSOA for our rack placement problem. The integer optimization model is applied dynamically based on a single-sample demand augmentation at each epoch. To avoid relying on distributional assumptions, we characterize the unknown demand distribution μ with an empirical distribution μ' obtained from historical data. We sample the size of each request and the power and cooling requirements from the empirical distributions given in Figure 1, assuming identical power and cooling requirements for all racks in the same demand request. One difference between the generic multi-stage stochastic optimization framework considered in this section and the rack placement problem is that the latter does not evolve in a well-specified finite horizon T ; rather, the horizon terminates when the data center can no longer accommodate incoming requests. Accordingly, we define a moving horizon in the SSOA algorithm: at each time period $t = 1, 2, \dots$, we sample requests for k_t periods, where k_t is determined so that future requests fill all non-empty rooms. We also adjust weights in the objective function to prioritize the placement of actual demand requests over sampled ones. Let \mathcal{A}^t denote the active requests (from previous time periods $1, \dots, t - 1$), \mathcal{D}^t the incoming requests at time t , and $\tilde{\mathcal{D}}^t$ the sample of k_t future demand arrivals. The algorithm determines the placement of incoming requests, using the online formulation (Equations (20)–(26)), until a request from the incoming batch \mathcal{D}^t gets rejected.

Finally, we also implement a “limited SSOA” method, which samples a handful of large demand requests at each iteration—three 20-rack and three 10-rack requests, in our experiments. Indeed, due to the complexity of our problem, even a single demand sample can significantly increase the computational requirements of the model. The limited SSOA approach aims to strike a balance between myopic decision-making (which is most computationally efficient) and the full SSOA application (which captures future demand at each batch).

Algorithm 2 SSOA implementation for the online rack placement problem.

for $t = 1, 2, \dots$ **do**

 Observe the current batch of requests \mathcal{D}^t .

 Sample $\tilde{\mathcal{D}}^t$ consisting of k_t i.i.d. future requests from the empirical distribution μ' .

 Solve the online rack placement formulation with active requests \mathcal{A}^t , incoming requests \mathcal{D}^t , and sampled requests $\tilde{\mathcal{D}}^t$ (Equations (20)–(26)).

 Implement decision $\mathbf{a}^t = \{u_{dg}^t : d \in \mathcal{D}^t, g \in \mathcal{G}\}$ and define \mathcal{A}^{t+1} accordingly.

If any demand request from \mathcal{D}^t is rejected based on action \mathbf{a}^t , **break**.

end for

6. Computational Results

We evaluate the rack placement models and algorithms in terms of solution quality and computational times. We implement our optimization methodology with various extents of batching (single-request batches, batch size of 5, batch size of 10), with and without the online objectives from Section 4.3 (row minimization, power surplus, and power balance), and with and without our SSOA approaches from Section 5.3 (no SSOA, limited SSOA, standard SSOA). For each solution, we report the number of successful placements relative to a perfect-information oracle based on omniscient demand knowledge, and in terms of stranded power (percentage of unused power versus power capacity). Together, these experiments quantify: (i) the benefits of batched optimization versus a one-request-at-a-time baseline; (ii) the benefits of online objectives in the integer optimization formulation; and (iii) the benefits of the SSOA algorithm versus a myopic optimization approach that does not account for future demand. All optimization models are solved with Gurobi using the JuMP package in Julia (Dunning et al. 2017), with a 10-minute limit per iteration.

We develop a simulation environment based on real-world data to replicate operations in large-scale data centers—as done in practice at Microsoft. The simulation starts with an empty data center, receives demand requests in batches, runs the optimization algorithms, and implements the rack placement solution. The simulation stops when the data center can no longer accommodate a full batch. Throughout, we consider a data center with two rooms each equipped with 36 rows. Each room features a three-level power hierarchy with four top-level UPS devices; each UPS device is connected to six PDU devices and each PDU device is connected to three PSU devices. We provide parameter values and simulation details in EC.1.2.

We use both sampled demand batches to define a controlled environment and identify the impact of key parameters, and actual demands from two data centers to estimate the potential impact of the methodology in practice. Sampled demand batches are obtained from historical distributions (Figure 1) using inverse transform sampling, with homogeneous power and cooling requirements

within each request. Even with real-world data, the simulation considers a stylized data center (e.g., empty initial configuration, 100% acceptance rate of the rack placement solutions). Thus, we complement simulation results with real-world deployment results in Section 7 to establish the impact of our solution in Microsoft’s data centers.

Value of rack placement optimization. Table 2 reports results from five simulations, with various extents of batching and each combination of the online objectives described in Section 4.3. Computational performance is measured in terms of runtimes (CPU) and optimality gap per iteration. To isolate the impact of the formulation, these results do not make use of SSOA.

The first row corresponds to a setting with a batch size of one and a myopic decision-making rule that treats one request at a time and does not anticipate future demand via the online objectives or the SSOA algorithm. This setting is the closest one to a simple decision-making rule that could be implemented in practice. However, even the one-request-at-a-time setting involves combinatorial complexities due to multi-rack requests, so it still represents a somewhat optimistic view of what can be typically achieved in the absence of an optimization methodology. In comparison to this one-request-at-a-time baseline, the results will therefore provide conservative estimates of the benefits of demand batching and of the online optimization methodology developed in this paper.

Table 2 Average solution and computational performance of the rack placement algorithm, without SSOA.

Batch Size	Online objectives		Placement %			Stranded Power %			Avg. Performance	
	Row	Power	Min.	Avg.	Max.	Min.	Avg.	Max.	CPU (s)	Gap (%)
1	✗	✗	86.00%	89.47%	92.16%	12.25%	14.50%	17.64%	0.09	0.00%
	✗	✓	89.91%	91.52%	95.10%	8.44%	12.36%	16.01%	0.35	0.00%
	✓	✗	83.33%	87.51%	90.83%	13.85%	16.30%	20.79%	0.28	0.00%
	✓	✓	88.17%	91.45%	93.00%	11.12%	12.65%	14.96%	0.52	0.00%
5	✗	✗	87.23%	90.72%	94.50%	10.40%	12.49%	14.96%	0.35	0.00%
	✗	✓	89.36%	91.91%	94.50%	8.42%	11.25%	13.02%	2.13	0.00%
	✓	✗	84.04%	88.55%	91.74%	12.25%	14.44%	17.25%	1.11	0.00%
	✓	✓	89.36%	91.71%	95.41%	8.66%	11.20%	13.02%	4.44	0.00%
10	✗	✗	89.72%	91.54%	94.50%	9.31%	11.12%	12.98%	0.86	0.00%
	✗	✓	90.65%	93.07%	96.33%	8.39%	9.46%	10.69%	10.74	0.01%
	✓	✗	82.24%	88.51%	93.58%	10.98%	13.57%	18.08%	35.25	0.00%
	✓	✓	91.59%	94.02%	97.25%	5.47%	7.61%	8.79%	138.70	0.01%

“Row”: row minimization objective. “Power”: power balance and surplus objectives. “CPU”: computational time. Results obtained with sampled demand batches, using the online rack placement algorithm without SSOA.

The first observation is the critical role of batched demand in rack placement optimization. With 10 requests per batch, the model improves placement rates by 2-3 percentage points and reduces stranded power by 3-5 percentage points on average versus the one-request-at-a-time benchmark. This result underscores the benefits of large-scale optimization to capture coupling requirements

across demand requests and data center resources, as compared to myopic strategies often used in practice. It is also consistent with our theoretical result in online bin packing (Theorem 2).

Next, the row minimization, power balance, and power surplus objectives are instrumental for improving the rack placement solution. Larger batch sizes yield improvements of another 3–4 percentage points, both in terms of utilization and power stranding. Interestingly, the worst performance occurs when we minimize rows (2–3% decrease in placement rates), suggesting that neglecting power consumption in favor of compact space allocations can create bottlenecks in power utilization. These results stress the importance of considering all our online objectives in tandem to achieve the best possible solutions. In particular, starting with a placement of 89.47% on average with a batch size of 1, the placement rate increases to 91.5% on average when increasing the batch size to 10 requests *or* when incorporating the online objectives; and when leveraging both batching and the online objectives, the algorithm further increases placement rates to 94% on average.

Value of SSOA. Table 3 incorporates our SSOA algorithm for the online rack placement problem—both the “standard” and “limited” SSOA implementations described in Section 5.3. We again consider various batch sizes, and implement the model with and without all online objectives.

Table 3 Average solution and computational performance of the rack placement algorithm, with SSOA.

Batch Size	Model		Placement %			Stranded Power %			Avg. Performance	
	SSOA	Objectives	Min.	Mean.	Max.	Min.	Mean.	Max.	CPU (s)	Gap (%)
1	None	✗	86.00%	89.47%	92.16%	12.25%	14.50%	17.64%	0.09	0.00%
		✓	88.17%	91.45%	93.00%	11.12%	12.65%	14.96%	0.52	0.00%
	Limited	✗	84.31%	91.00%	95.41%	8.48%	12.44%	17.52%	0.24	0.00%
		✓	90.20%	92.63%	95.41%	8.48%	10.93%	13.39%	10.00	0.00%
	Standard	✗	91.40%	93.63%	95.10%	8.44%	9.55%	10.69%	63.85	0.02%
		✓	94.00%	95.45%	97.06%	6.96%	8.27%	9.82%	313.77	0.10%
5	None	✗	87.23%	90.72%	94.50%	10.40%	12.49%	14.96%	0.35	0.00%
		✓	89.36%	91.71%	95.41%	8.66%	11.20%	13.02%	4.44	0.00%
	Limited	✗	89.36%	91.53%	94.50%	10.00%	11.28%	12.59%	1.42	0.00%
		✓	95.15%	96.26%	98.17%	5.47%	6.72%	8.20%	63.79	0.01%
	Standard	✗	92.16%	94.34%	96.12%	6.96%	8.56%	10.40%	46.00	0.00%
		✓	95.15%	96.14%	97.87%	5.47%	7.02%	8.48%	289.56	0.04%
10	None	✗	89.72%	91.54%	94.50%	9.31%	11.12%	12.98%	0.86	0.00%
		✓	91.59%	94.02%	97.25%	5.47%	7.61%	8.79%	138.70	0.01%
	Limited	✗	91.26%	93.24%	97.25%	5.59%	8.63%	12.39%	7.07	0.00%
		✓	92.52%	95.95%	98.17%	4.61%	5.88%	6.96%	142.09	0.01%
	Standard	✗	88.66%	93.23%	98.13%	4.08%	9.04%	14.27%	66.15	0.00%
		✓	92.52%	95.56%	98.17%	5.17%	6.01%	6.96%	276.41	0.03%

“Objectives”: row minimization, power balance, and power surplus. Same nomenclature as in Table 2 otherwise.

The results show the strong benefits of SSOA over a simpler re-optimization approach that does not sample future demand requests. Without the online objectives, SSOA increases average placement rates by 2–4 percentage points and decreases average power stranding by 2–5 percentage points. With the online objectives, SSOA improves the final placement rates and power stranding by

4–6 percentage points. Recall from Table 2 that the online objectives alone increase placement rates by 2–3 percentage points and decrease power stranding by 1–3 percentage points. In other words, SSOA can be highly valuable by itself, yielding comparable and even stronger benefits than the row minimization, power balance, and power surplus metrics. Most importantly, the best outcomes are obtained by leveraging both the online objectives and the SSOA methodology, thereby underscoring their joint role toward optimizing online rack placement decisions under demand uncertainty.

Perhaps more surprisingly, the SSOA algorithm provides comparable benefits to demand batching. As expected, the benefits of SSOA are stronger in the absence of batching because the cost of myopic decision-making is much stronger in that case. However, the quality of the SSOA solution is similar with demand batches of 1, 5 or 10, both on average and in the worst case. This observation suggests that the SSOA algorithm may be sufficient to alleviate the pitfalls of one-request-at-a-time decision-making, even without batching. From a practical standpoint, the SSOA algorithm therefore provides a simple and generalizable approach that can generate high-quality solutions in cases where batching is not possible or expensive—due, for instance, to service delays.

Moreover, the “limited” SSOA algorithm defines a middle ground between the no-SSOA and standard SSOA solutions. Specifically, it achieves intermediate solutions with small demand batches in much faster computational times; and it is competitive with SSOA when demand batches are larger. These results further underscore the impact of capturing even limited information on future demand requests at each iteration, and suggest opportunities to deploy computationally efficient algorithms that can ultimately generate high-quality rack placement solutions.

Additional findings. Figure 4 depicts resource utilization over time for five solutions: (i) the “offline” model with no online objectives and no SSOA; (ii) the model with the row-minimization objective; (iii) the model with the power surplus and power balance objectives; (iv) the model with all online objectives; and (v) the model with all online objectives and SSOA. The figure reports the cumulative number of used rows normalized against the number of rows in each room (metric linked with the row-minimization objective), as well as power imbalance and power surplus normalized against perfectly balanced UPS pair load (metrics linked with the power objectives). We conservatively use a batch size of 10, for which the offline model performs best.

Figure 4 highlights how the online objectives and SSOA coordinate to optimize rack placements by conserving data center resources over time. In fact, it also uncovers the importance of jointly considering space- and power-related objectives in online rack placement for leaner resource management. In this example, the row-minimization objective alone consolidates demands onto fewer rows but deteriorates the management of failover power capacity (linked with high power imbalance in Room 2). The figure also reinforces the joint role of the online objectives and the SSOA algorithm toward maximizing data center utilization without overloading power resources.

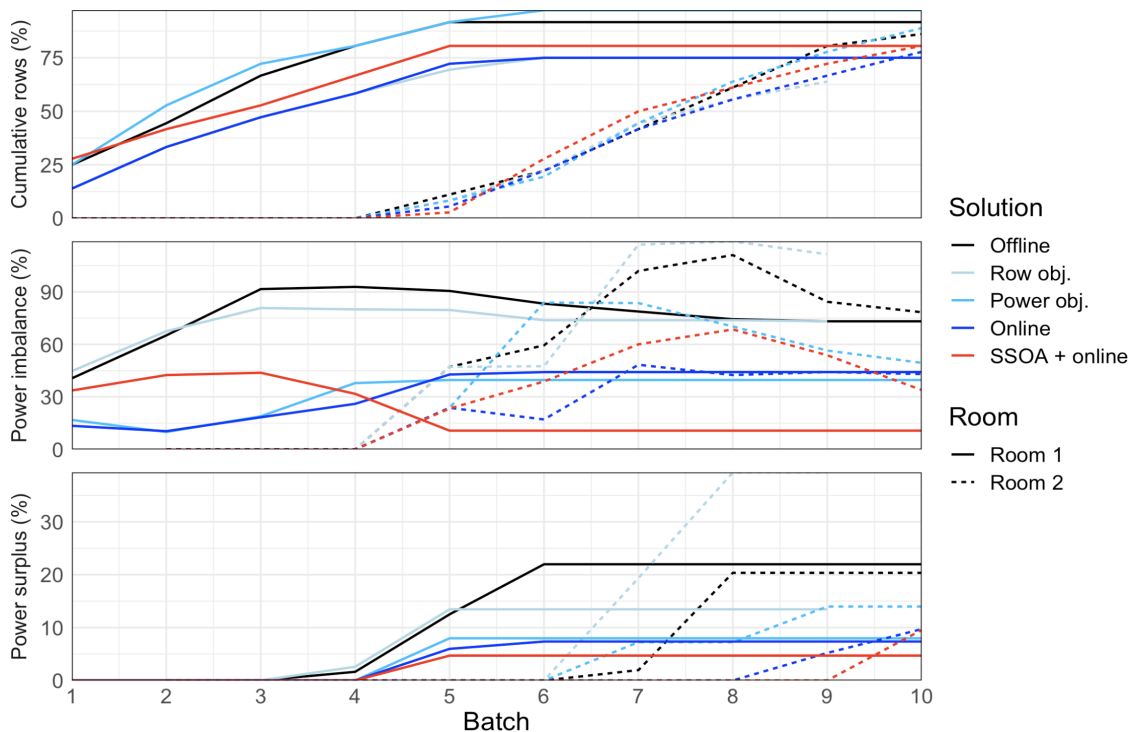


Figure 4 Evolution of space and power utilization, in one instance from Tables 2 and 3 with a batch size of 10. In order, the stranded power for each trial is 11.93%, 18.08%, 10.69%, 8.79%, and 6.96%; and the placement rate for each trial is 89.72%, 82.24%, 90.65%, 91.59%, and 92.52%.

Figure 5 reports similar results as in Tables 2 and 3 using demand data from two sample data centers. As opposed to considering controlled demand batches, these experiments consider actual—and heterogeneous—batches obtained from historical data. The observations are very similar to the earlier ones, showing the potential of the methodology in practice. In particular, the combination of the online optimization objectives and the SSOA algorithm results in a joint improvement in data center utilization (+3–5% in rack placements) and power consumption (reduction in power stranding by 3–4 percentage points, representing a relative 50% reduction).

In conclusion, the computational results reported in this section complement our theoretical guarantees by highlighting the benefits of our optimization methodology for online rack placement. As compared to a typical re-optimization approach that treats one request at a time without anticipating future demand, the online integer optimization formulation and the SSOA algorithm can both increase data center utilization by up to 5% and can halve stranded power while satisfying reliability requirements. These gains translate into significant financial and environmental impact, which motivates the deployment of our solution in practice across Microsoft’s fleet of data centers.

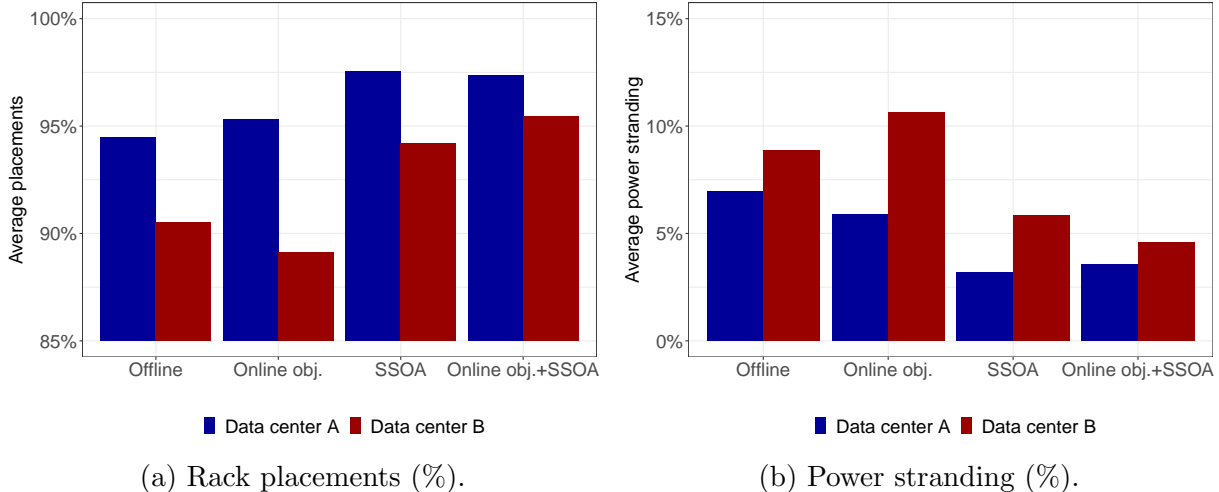


Figure 5 Computational results on placements and power stranding using data from two sample data centers. “Offline” corresponds to the model without the online objectives and without SSOA.

7. Real-world Impact in Microsoft Data Centers

Recall that rack placement decisions relied primarily on the expertise of data center managers, assisted by simple spreadsheet tools and feasibility-oriented software. The growth of cloud computing has rendered these decisions increasingly complex, creating many interdependent considerations and conflicting objectives. To alleviate high mental loads and operational inefficiencies, we have deployed our rack placement solution in hundreds of Microsoft’s data centers worldwide. The overarching objective was to combine the strength of the optimization methodology and of human expertise, by building an effective decision support tool but leaving decision-making authority to data center managers. We have extensively collaborated with several stakeholder groups to iteratively improve the solution and gradually deploy it across the organization (Section 7.1). As a result, the software’s recommendations were increasingly adopted by data center managers, leading to reductions in power stranding and significant cost savings (Section 7.2). The success of this deployment underscores the impact of human-machine interactions in cloud supply chains to turn an optimization prototype into a full-scale software solution deployed in production.

7.1. Solution Deployment in Microsoft’s Fleet of Data Centers

Software development. We packaged our model and algorithm into a software tool that could be embedded into the production ecosystem. We built data pipelines to get access to real-time information on incoming demand and data center utilization. Each demand batch triggers our optimization algorithm to generate placement suggestions. To ensure acceptable wait times for data center managers, we currently impose a four-minute time limit for each optimization run—strengthening the benefits of our SSOA algorithm as compared to more complex multi-stage stochastic optimization algorithms such as sample average approximation. We developed a user interface enabling data

center managers to visualize placement suggestions in the data center (Figure 6a shows a sample visualization). For each request, data center managers can either accept the placement suggestion, or reject it and select their own placement. The suggested and final placements are both recorded.

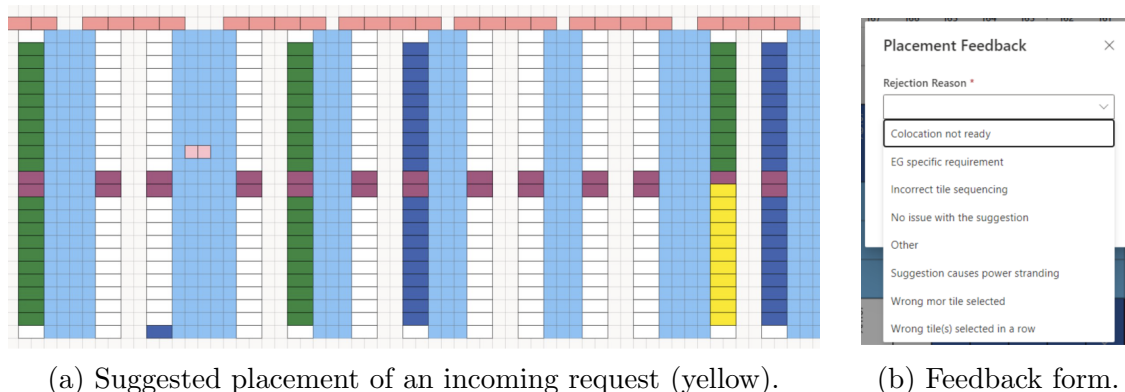


Figure 6 User interface for data center managers at the core of our solution deployment.

Pilot. After extensive simulations and testing, we initiated a small-scale pilot in 13 data centers. This phase started at the end of 2021 and lasted three months. We fostered direct interactions with data center managers to assess the new solution. Initial feedback helped us identify issues in the data pipelines. For instance, early deployments failed to record that some rooms were unavailable, that some rows were already reserved, and that some requests came with placement restrictions.

To continue gathering feedback toward full-scale deployment, we augmented the user interface for data center managers to specify the reason for each placement rejection (Figure 6b). This new deployment phase provided valuable insights on real-time adoption. We devised a principled approach to analyze feedback by grouping the main rejection reasons into several categories, including: (i) engineering group requirements; (ii) power balancing considerations; (iii) conflicts with other requests (“already reserved”); (iv) availability of better placements by throttling lower-priority demands (“multi-availability”); and (v) opportunities to utilize small pockets of space (“better space packing”). These options were supplemented with a free-text “Other” category, mainly used to specify ad hoc requests, hardware compatibility issues, and software bugs.

Full-scale deployment. We organized information sessions to familiarize data center managers with the new system and demonstrate its capabilities. These sessions were well received, and data center managers showed great interest in the details of the model. Within a month, our solution was launched globally across Microsoft’s global fleet of hundreds of data centers. Since then, we performed modeling adjustments to improve the quality of rack placement recommendations, using data on the rejection reasons (Figure 6b). For instance, we increased the value of the λ_m parameters in the objective function to further disincentivize opening new rooms and therefore ease operational

overhead, and we expanded the model to satisfy common requirements from engineering groups (e.g., co-locating certain demand requests on the same row).

Figure 7 reports the main rejection reasons in the last quarter of 2022 and the second quarter of 2023. Once our modeling adjustments got implemented, tested and deployed in production in early 2023, the incidence of rejections due to engineering group requirements decreased from over 40% to less than 20%. The remaining engineering group requirements are mostly driven by one rack type, which currently lies out of scope of the model. Thus, the iterative modeling adjustments enabled to address the main issues and increase overall adoption of the rack placement solution.

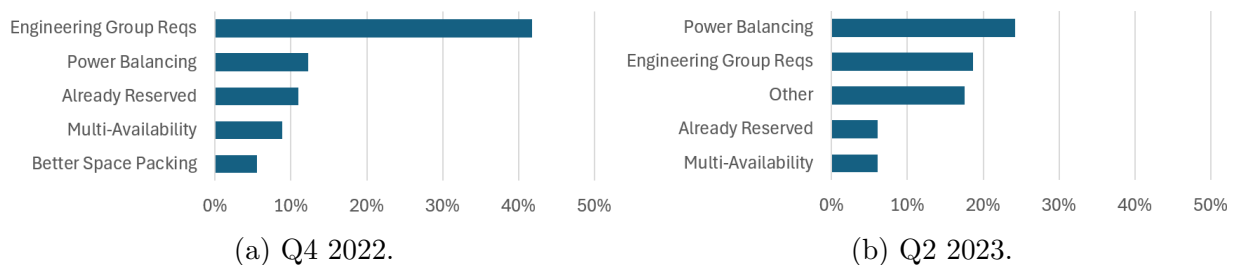


Figure 7 Rejection reasons before and after incorporating engineering group requirements in the optimization.

Takeaways. We had to overcome multiple challenges to enable full-scale deployment. The first one involved *solving the right problem*. In practice, there is no “clean” problem description outlining objectives and constraints that can be directly translated into an optimization framework. We devoted significant time and effort to understand the rack placement process in detail, in close collaboration with domain experts and stakeholders (e.g., data center managers, program managers, engineering groups). The second one involved *data challenges*. To overcome inconsistencies between databases, we had to build dedicated data pipelines into our optimization model. We also developed user interfaces to make the optimization solutions available to key decision-makers in real time and collect data on adoption. A third challenge was *human factors*: to replace an existing (mostly manual) system with a sophisticated optimization approach, it was critical to involve data center managers early on and gain their trust. This allowed us to leverage their expertise and feedback to strengthen the optimization solution. At the same time, this enabled them to better understand the logic behind the new rack placement system, thereby alleviating the pitfalls of “black-box” optimization. The working sessions were particularly useful to make the model-based recommendation more interpretable and transparent. Ultimately, our full-scale optimization deployment highlights the importance of keeping the user’s perspective in mind when designing real-world optimization solutions through cross-organizational collaborations at the human-machine interface.

7.2. Impact: Benefits of the Solution in Practice

Adoption. Figure 8 reports the monthly *acceptance ratio* across all Microsoft data centers in April–July 2023, defined as the proportion of placement recommendations that were accepted by data center managers. Given the deep domain expertise of data center managers, the acceptance ratio is a good indicator of the quality of the recommendation. During this period, our solution was continuously deployed in all data centers but we made two significant improvements. First, we incorporated the preference from engineering groups to distribute power across different rooms, by penalizing placements that would exceed a “power budget” for each engineering group in each room. This change was deployed in production in May 2023. Second, we augmented our solution in June 2023 to support a particular data center architecture called *Flex* (studied in detail by Zhang et al. 2021), which can throttle low-priority demands in case of failover.

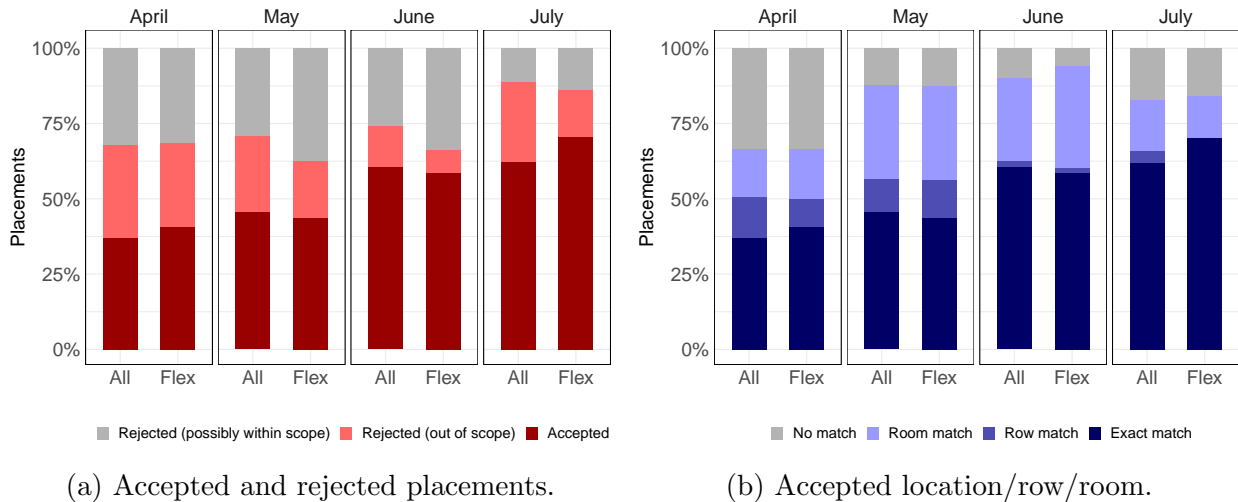


Figure 8 Acceptance of our recommendations by the data center managers.

Figure 8a shows a strong increase in accepted requests between April 2023 and July 2023. In fact, these results show that the deployment of an optimization tool does not necessarily lead to immediate large-scale impact. Rather, adoption increases over time as users get progressively more familiar with the tool, and as the algorithm gets improved to capture practical requirements. In our case, the acceptance ratio increased from 35% in April 2023 to over 60% in July 2023 across all Microsoft data centers—and to over 70% among the Flex data centers in particular. In fact, Figure 8b shows that, even when the data center managers rejected the specific recommendation from our solution, many placements remained in the same room and even in the same row. In particular, the room recommended by our solution was accepted for 80–90% of placements.

Figure 8a also breaks down rejected requests into those out of the scope of the optimization model and those possibly within scope. Out-of-scope rejections are primarily due to data issues and bugs

(indicated, for instance, in the “already reserved” and “other” categories of the feedback form). Such rejections could be addressed over time as data pipelines mature. The remaining rejections include requests for which the solution provided an appropriate recommendation but the data center managers decided for other placements. Such rejections would require deeper changes to the optimization model. This breakdown suggests that the vast majority of rejections at the end of the deployment period fell out of scope, suggesting that our iterative improvements were successful at addressing the main in-scope issues. Ultimately, when disregarding out-of-scope rejections, the potential of our optimization solution reaches 80-90% of requests across all data centers.

Altogether, these results suggest that our optimization model and algorithm yielded high-quality placement recommendations. Thanks to extensive deployment efforts, these recommendations were implemented most of the time by the data center managers. Next, we evaluate the impact of these placements on power stranding—the main bottleneck of data center operations.

Power stranding. We gathered data from monthly power stranding reports compiled by the production team between October 2022 and September 2023. These reports contain the power stranding percentage (percentage of total power that cannot be used to serve cloud demand) for each data center at the beginning of each month. Note that it is difficult to isolate the impact of our optimization solution, as power stranding depends on overall utilization within each data center, its configuration, and data centers’ broader operations. To overcome this challenge, we use the acceptance ratio as an estimate of the prevalence of our algorithm vs. human decision-making in the data center. We use a threshold of 60% to classify a data center as high vs. low acceptance ratio, distinguishing the top quartile from the bottom three quartiles.

As a baseline, the top figure reports the distribution of power stranding across all data centers in October 2022. The bottom figures provide corresponding pictures across all data centers and across Flex data centers in September 2023. All these figures distinguish data centers with high vs. low acceptance rates of our solution.

The two sets of data centers were fairly homogeneous in October 2022 prior to the deployment of our solution, with an average power stranding of 4.4–4.6% and a similar distribution. A year later, they feature sharp differences: average power stranding decreased in data centers with a high acceptance ratio (down to 3.91%) but increased in those with a low acceptance ratio (up to 5.37%). The decrease can be surprising as data center utilization generally grows over time, but can be explained by occasional changes in data center configurations as requests get decommissioned and as data center managers manually alter some rack placements. Then, our optimization solution improved power utilization between data centers with high vs. low acceptance ratios, as indicated by a 10-30% difference in power stranding—or a 1-1.5 percentage point difference—while adhering to high levels of service reliability captured by the redundancy requirements.

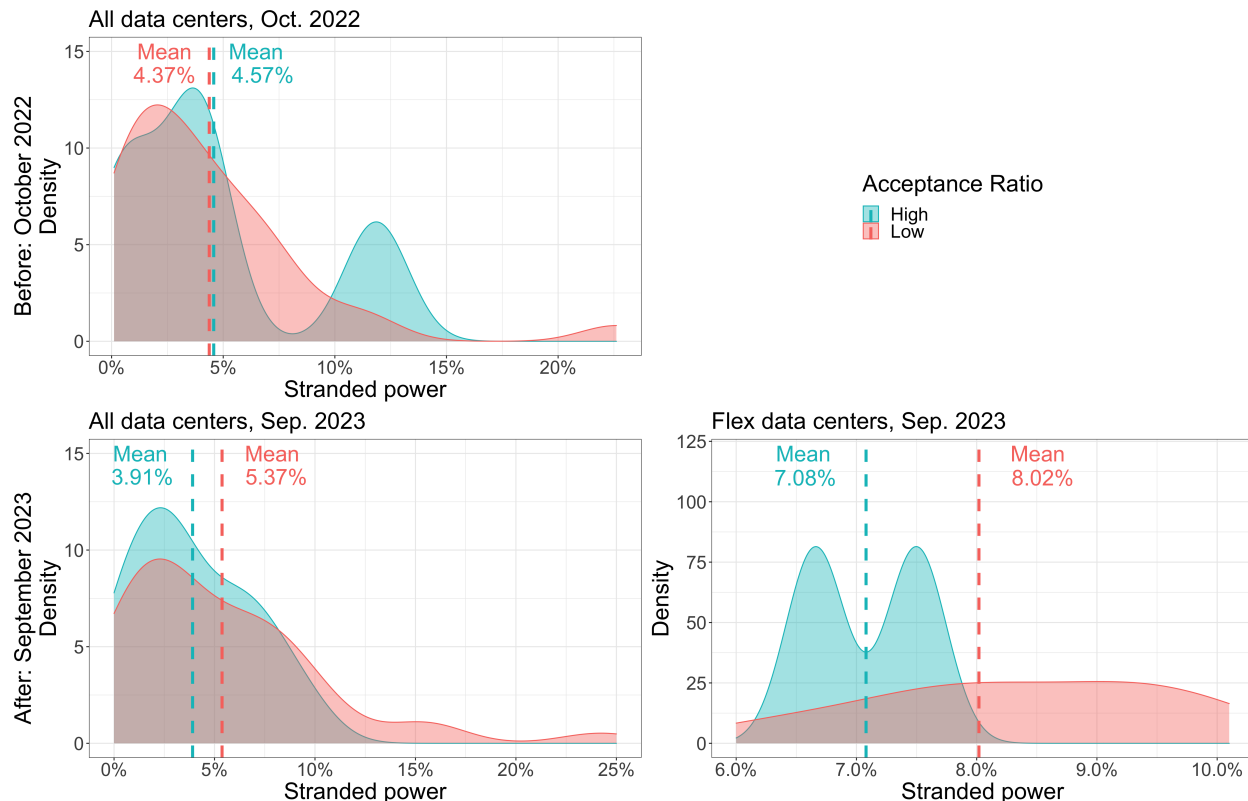


Figure 9 Power stranding density plots and mean values for datacenters with high and low acceptance ratios.

Given the scale of cloud computing, a 1% improvement in power utilization can avoid building unnecessary new data center capacity, resulting in strong efficiency and sustainability gains for global cloud supply chains. Based on post-deployment evidence, the solution in production is leading to multi-million-dollar cost savings across Microsoft’s fleet of data centers. Specifically, given a \$6.4-\$13.4 data center construction cost per Watt ([Statista 2023](#)) and Microsoft’s multi-GW fleet ([Data Center Knowledge 2023](#)), a percentage point decrease in power stranding can lead to savings on the order of hundreds of millions of dollars, along with reductions in greenhouse gas emissions on the order of hundreds of thousands of tons of CO₂ equivalents. Although these numbers are approximate due to the difficulties of isolating our solution, results suggest a significant impact on data center operations toward more efficient, reliable and sustainable cloud supply chains.

8. Conclusion

This paper optimizes rack placement recommendations to maximize utilization in large-scale data centers while minimizing operational complexity and managing coupled availability constraints across space, power, and cooling resources. We implemented an online version of the model over a rolling horizon, paired with dedicated objectives to pace resource utilization over time for

future demand. We proposed a single-sample online approximation (SSOA) algorithm as an easily-implementable and generalizable approach to multi-stage stochastic optimization. The algorithm relies on a single-realization approximation of uncertainty, along with online re-optimization. We provided theoretical performance guarantees of SSOA in canonical bin packing and generalized assignment settings, motivating its application to the online rack placement problem.

Computational results showed that the modeling and algorithmic approach can provide significant benefits by increasing rack placement rates and reducing power stranding. In turn, we packaged the optimization model and algorithm into a dedicated decision-support software tool to deploy it across Microsoft’s data centers, in close collaboration with data center managers. Recent usage data suggest that our approach led to high adoption by data center managers and to a significant reduction in power stranding as a result. These improvements can translate into very large cost savings along with a concomitant reduction in greenhouse gas emissions. At a time when cloud computing is growing into a major component of modern supply chains, this paper contributes new models, algorithms, and practical evidence toward the optimization of data center operations.

Acknowledgments

This work was partially supported by the MIT Center for Transportation and Logistics UPS PhD Fellowship.

References

- Arbaban ME, Chen S, Moizadeh K (2021) Capacity expansions with bundled supplies of attributes: An application to server procurement in cloud computing. *Manufacturing & Service Operations Management* 23(1):191–209.
- Arlotto A, Gurvich I (2019) Uniformly bounded regret in the multisecretary problem. *Stochastic Systems* 9(3):231–260.
- Azar PD, Kleinberg R, Weinberg SM (2014) Prophet inequalities with limited information. *Proceedings of the twenty-fifth annual ACM-SIAM symposium on Discrete algorithms*, 1358–1377 (SIAM).
- Banerjee S, Freund D (2019) Good prophets know when the end is near. *Available at SSRN 3479189* .
- Barroso LA, Hölzle U, Ranganathan P (2019) *The datacenter as a computer: Designing warehouse-scale machines* (Springer Nature).
- Bertsekas D (2012) *Dynamic programming and optimal control: Volume I*, volume 4 (Athena scientific).
- Bertsimas D, Mundru N (2022) Optimization-based scenario reduction for data-driven two-stage stochastic optimization. *Operations Research* .
- Besbes O, Mouchtaki O (2023) How big should your data really be? data-driven newsvendor: learning one sample at a time. *Management Science* .
- Birge JR, Louveaux F (2011) *Introduction to stochastic programming* (Springer Science & Business Media).

- Buchbinder N, Fairstein Y, Mellou K, Menache I, Naor JS (2022) Online virtual machine allocation with lifetime and load predictions. *SIGMETRICS Perform. Eval. Rev.* 49(1):9–10.
- Bumpensanti P, Wang H (2020) A re-solving heuristic with uniformly bounded loss for network revenue management. *Management Science* 66(7):2993–3009.
- Caramanis C, Dütting P, Faw M, Fusco F, Lazos P, Leonardi S, Papadigenopoulos O, Pountourakis E, Reiffenhäuser R (2022) Single-sample prophet inequalities via greedy-ordered selection. *Proceedings of the 2022 Annual ACM-SIAM Symposium on Discrete Algorithms (SODA)*, 1298–1325 (SIAM).
- Chen S, Moinzadeh K, Song JS, Zhong Y (2023) Cloud computing value chains: Research from the operations management perspective. *Manufacturing & Service Operations Management* 25(4):1338–1356.
- Cheung WC, Simchi-Levi D (2019) Sampling-based approximation schemes for capacitated stochastic inventory control models. *Mathematics of Operations Research* 44(2):668–692.
- Cohen MC, Keller PW, Mirrokni V, Zadimoghaddam M (2019) Overcommitment in cloud services: Bin packing with chance constraints. *Management Science* 65(7).
- Data Center Knowledge (2023) 2023: These Are the World’s 12 Largest Hyperscalers. <https://www.datacenterknowledge.com/manage/2023-these-are-world-s-12-largest-hyperscalers>.
- Dayarathna M, Wen Y, Fan R (2016) Data center energy consumption modeling: A survey. *IEEE Communications Surveys & Tutorials* 18(1):732–794.
- Dunning I, Huchette J, Lubin M (2017) JuMP: A modeling language for mathematical optimization. *SIAM review* 59(2):295–320.
- Fan X, Weber WD, Barroso LA (2007) Power provisioning for a warehouse-sized computer. *SIGARCH Comput. Archit. News* 35(2):13–23.
- Freund D, Zhao J (2021) Overbooking with bounded loss. *Proceedings of the 22nd ACM Conference on Economics and Computation*, 477–478.
- Gardner K, Harchol-Balter M, Scheller-Wolf A, Velednitsky M, Zbarsky S (2017) Redundancy-d: The power of d choices for redundancy. *Operations Research* 65(4):1078–1094.
- Grosz I, Scully Z, Harchol-Balter M, Scheller-Wolf A (2022) Optimal scheduling in the multiserver-job model under heavy traffic. *Proceedings of the ACM on Measurement and Analysis of Computing Systems* 6(3):1–32.
- Gupta A, Molinaro M (2016) How the experts algorithm can help solve LPs online. *Mathematics of Operations Research* 41(4):1404–1431.
- Gupta V, Radovanovic A (2020) Interior-point-based online stochastic bin packing. *Operations Research* 68(5):1474–1492.
- Gutin G, Jensen T, Yeo A (2005) Batched bin packing. *Discrete Optimization* 2(1):71–82.

- Harchol-Balter M (2013) *Performance modeling and design of computer systems: queueing theory in action* (Cambridge University Press).
- International Energy Agency (2022) Infrastructure deep dive: Data centres and data transmission networks. Technical report.
- Jasin S, Kumar S (2012) A re-solving heuristic with bounded revenue loss for network revenue management with customer choice. *Mathematics of Operations Research* 37(2):313–345.
- Kleywegt AJ, Shapiro A, Homem-de Mello T (2002) The sample average approximation method for stochastic discrete optimization. *SIAM Journal on optimization* 12(2):479–502.
- Levi R, Perakis G, Uichanco J (2015) The data-driven newsvendor problem: New bounds and insights. *Operations Research* 63(6):1294–1306.
- Li D, Guo C, Wu H, Tan K, Zhang Y, Lu S, Wu J (2011) Scalable and cost-effective interconnection of data-center servers using dual server ports. *IEEE/ACM Transactions on Networking* 19(1):102–114.
- Li Y, Tang X, Cai W (2015) Dynamic bin packing for on-demand cloud resource allocation. *IEEE Transactions on Parallel and Distributed Systems* 27(1):157–170.
- Liu M, Tang X (2022) Dynamic bin packing with predictions. *Proc. ACM Meas. Anal. Comput. Syst.* 6(3), URL <http://dx.doi.org/10.1145/3570605>.
- Liu RP, Mellou K, Gong XY, Li B, Coffee T, Pathuri J, Simchi-Levi D, Menache I (2023) Efficient cloud server deployment under demand uncertainty. Available at SSRN 4501810 .
- Lodi A, Martello S, Vigo D (2002) Recent advances on two-dimensional bin packing problems. *Discrete Applied Mathematics* 123(1):379–396.
- Lyu J, You M, Irvine C, Jung M, Narmore T, Shapiro J, Marshall L, Samal S, Manousakis I, Hsu L, Subbarayalu P, Raniwala A, Warriar B, Bianchini R, Shroeder B, Berger DS (2023) Hyrax: Fail-in-place server operation in cloud platforms. *Proceedings of the 17th Symposium on Operating Systems Design and Implementation (OSDI)* (USENIX).
- Maglaras C, Meissner J (2006) Dynamic pricing strategies for multiproduct revenue management problems. *Manufacturing & Service Operations Management* 8(2):136–148.
- Mellou K, Molinaro M, Zhou R (2023) Online Demand Scheduling with Failovers. *50th International Colloquium on Automata, Languages, and Programming (ICALP 2023)*, volume 261, 92:1–92:20.
- Muir C, Marshall L, Toriello A (2024) Temporal bin packing with half-capacity jobs. *INFORMS Journal on Optimization* 6(1):46–62.
- National Resources Defense Council (2014) Data center efficiency assessment. Technical report.
- Perez-Salazar S, Singh M, Toriello A (2022) Adaptive bin packing with overflow. *Operations Research Articles in Advance*.

- Powell WB (2022) *Reinforcement Learning and Stochastic Optimization: A Unified Framework for Sequential Decisions* (John Wiley & Sons).
- Radovanović A, Koningstein R, Schneider I, Chen B, Duarte A, Roy B, Xiao D, Haridasan M, Hung P, Care N, et al. (2022) Carbon-aware computing for datacenters. *IEEE Transactions on Power Systems* 38(2):1270–1280.
- Rhee WT, Talagrand M (1993a) On-line bin packing of items of random sizes, II. *SIAM Journal on Computing* 22(6):1251–1256.
- Rhee WT, Talagrand M (1993b) On line bin packing with items of random size. *Mathematics of Operations Research* 18(2):438–445.
- Römisch W (2009) Scenario reduction techniques in stochastic programming. *International Symposium on Stochastic Algorithms*, 1–14 (Springer).
- Rubinstein A, Wang JZ, Weinberg SM (2019) Optimal single-choice prophet inequalities from samples. *arXiv preprint arXiv:1911.07945* .
- Schroeder B, Wierman A, Harchol-Balter M (2006) Closed versus open system models: a cautionary tale. *Network System Design and Implementation* .
- Secomandi N (2008) An analysis of the control-algorithm re-solving issue in inventory and revenue management. *Manufacturing & Service Operations Management* 10(3):468–483.
- Srinivasan V, Thompson GL (1973) An algorithm for assigning uses to sources in a special class of transportation problems. *Operations Research* 21(1):284–295.
- Statista (2022) Statista Market Insights - Public Cloud. Technical report.
- Statista (2023) Data center markets worldwide ranked by cost of data center construction in 2023. <https://www.statista.com/statistics/1106621/global-data-center-markets-ranked-by-cost-of-construction/>.
- Sutton RS, Barto AG (2018) *Reinforcement learning: An introduction* (MIT press).
- Uptime Institute (2014) Data center site infrastructure tier standard: Operational sustainability. Technical report, <http://uptimeinstitute.com/publications>.
- Van Der Vaart AW, Wellner JA (1996) *Weak convergence and empirical processes: with applications to statistics* (Springer New York).
- Vera A, Banerjee S (2021) The bayesian prophet: A low-regret framework for online decision making. *Management Science* 67(3):1368–1391.
- Wang Y, Wang H (2022) Constant regret resolving heuristics for price-based revenue management. *Operations Research* 70(6):3538–3557.
- Wu Q, Deng Q, Ganesh L, Hsu CH, Jin Y, Kumar S, Li B, Meza J, Song YJ (2016) Dynamo: Facebook’s data center-wide power management system. *ACM SIGARCH Computer Architecture News* 44(3):469–480.

-
- Xu H, Li B (2013) Joint request mapping and response routing for geo-distributed cloud services. *2013 Proceedings IEEE INFOCOM*, 854–862.
- Zhang C, Kumbhare AG, Manousakis I, Zhang D, Misra PA, Assis R, Woolcock K, Mahalingam N, Warriar B, Gauthier D, et al. (2021) Flex: High-availability datacenters with zero reserved power. *2021 ACM/IEEE 48th Annual International Symposium on Computer Architecture (ISCA)*, 319–332 (IEEE).
- Zhang W, Wang K, Jacquillat A, Wang S (2023) Optimized scenario reduction: Solving large-scale stochastic programs with quality guarantees. *INFORMS Journal on Computing* .
- Zou S, Zhang Q, Yue C, Du S (2021) Effect of servers' arrangement on the performance of a loop thermosyphon system used in data center. *Applied Thermal Engineering* 192:116955.

Online Rack Placement in Large-Scale Data Centers

Electronic Companion

EC.1. Additional Details on the Rack Placement Model

EC.1.1. Online Objectives

In Section 4, we used the objectives of row minimization, power surplus and power balance in the online rack placement model to pace the utilization of data center resources for future demand. We provide in this appendix some details on the motivation underlying these modeling choices.

Row minimization. Consider a simple example with an initially empty data center that comprises 10 rows with 20 tiles each. Suppose that the first batch of demand requests includes 10 requests of 10 tiles each. Without row minimization, the 10 requests could all be assigned to different rows, leading to 10 partially utilized rows. If the next batch consists of five 20-rack requests, then none of these requests can be feasibly placed in the data center. By minimizing the number of used rows, the initial 10 requests would consume only five rows, allowing the upcoming batch of large requests to be successfully placed on the remaining five rows.

Power balance and power surplus. For simplicity, we focus here on UPS devices, which are typically the main bottlenecks in a data center’s power hierarchy. Consider a single-room data center with a power hierarchy consisting of 4 UPS devices (see Figure 2b), each with a regular capacity of 180W and a failover capacity of 240W. Thus, the data center can accommodate a load of 720W. Assume that the room operates at capacity and that the power load has been perfectly balanced across all pairs of UPSs (1-2, 1-3, 1-4, 2-3, 2-4, and 3-4), so that each of the six pairs of UPSs handles a load of $\frac{720}{6} = 120$ W. This power allocation fulfills the capacities of the UPS devices under regular conditions: each UPS appears in three pairs and handles half the corresponding load, so each UPS handles a load of $120 \times 3/2 = 180$ W. The power allocation also fulfills the capacities of the UPS devices under failover conditions: if one UPS fails, each of the surviving UPS devices handles the full load for the corresponding pair and continues to share the load on the other two pairs, so each UPS device handles a load of $120 \times 2/2 + 120 = 240$ W. In this case, the perfectly-balanced load achieves full utilization of the data center’s power budget.

Assume now that one of the UPS pairs (e.g., UPS 1 and UPS 2) has exceeded the perfectly balanced allocation of 120W by some amount $\varepsilon > 0$. To accommodate the failover capacity of UPS 1 in case UPS 2 fails, the total power handled by the remaining pairs of UPS 1 (i.e., UPS pairs 1-3 and 1-4) must not exceed $240 - 2\varepsilon$. Symmetrically, UPS pairs 2-3 and 2-4 must not handle more than $240 - 2\varepsilon$ to respect UPS 2’s failover capacity if UPS 1 fails. Finally, UPS pair 3-4 can handle up to $120 + \varepsilon$ to satisfy their own capacities. Therefore, the power utilization is at most $720 - 2\varepsilon$, leading to at least 2ε units of power stranding.

Motivated by these observations, the row minimization objective consolidates small requests on fewer rows to leave large slots available for future requests, the power surplus objective penalizes power allocations to UPS pairs that exceed their perfectly-balanced target load, and the power balance objective promotes balanced loads across UPS pairs by minimizing the largest power load difference across all pairs.

EC.1.2. Parameter Values

In our experiments, we use a value of λ_m equal to 40, 3 and 0 for rooms up to 0%, 20%, 100% full, respectively; and we use a value of θ_r equal to 2, 1 and 0 for rows up to 0%, 50%, 100% full, respectively. We use a reward for each placement of $\mu = 200$, and objective weights of $\alpha = 10^{-5}$, $\beta = 10^{-3}$, $\tau = 1$. In the online SSOA model, the demand placement rewards μ must be indexed by each demand to prioritize the placement of real demands over sampled demands. In particular, we exclude placing sampled demands in empty rooms; and we avoid opening a new room to make space in existing rooms for all sampled demands and relegating actual demands to the new room.

In our simulations, the top-level UPS devices have regular capacities equal to 75% of their failover capacities. The regular capacity of each mid-level PDU and leaf-level PSU is respectively 20% and 60% of their parent's capacity. Finally, the failover capacities of the PDU and PSU devices is twice as large as their regular capacities.

EC.2. Multi-dimensional Generalized Assignment

Multi-dimensional generalized assignment is a special case of a more general packing problem.

DEFINITION EC.1 (STOCHASTIC PACKING PROBLEM). Items arrive one at a time, indexed by $t = 1, \dots, T$. For each item, an action needs to be taken out of m possibilities, which we capture with decision variables $x^t \in \Delta_I := \{\mathbf{0}, \mathbf{e}_1, \dots, \mathbf{e}_m\} \subseteq \mathbb{R}^m$ (where $\mathbf{0}$ denotes the zero vector and \mathbf{e}_i denotes the vector with a one in the i -th component and zeros elsewhere). The problem features d resources, with capacity b_j for resource $j = 1, \dots, d$. The i -th action for item $t = 1, \dots, T$ comes with an unknown value $C_i^t \geq 0$ and consumes an unknown amount $A_{ij}^t \geq 0$ of resource $j = 1, \dots, d$. Both of these quantities are only revealed when the item arrives, and remain unknown for future items. For item t , we define the value vector $C^t = (C_1^t, \dots, C_m^t)$, the resource requirements matrix $A^t = (A_{ij}^t)_{ij}$, and the vector of the j -th resource requirements $A_j^t = (A_{1j}^t, \dots, A_{mj}^t)$. We also denote the resource vector $b = (b_1, \dots, b_d)$. The tuples (C^t, A^t) are drawn independently from a joint distribution μ . The reward function is given by:

$$\text{reward}(x^1, \dots, x^T; C^1, \dots, C^T, A^1, \dots, A^T) = \begin{cases} \sum_{t=1}^T \sum_{i=1}^m C_i^t x_i^t & \text{if } \sum_{t=1}^T \sum_{i=1}^m A_{ij}^t x_i^t \leq b_j, \forall j = 1, \dots, d \\ & \text{and } \sum_{i=1}^m x_i^t \leq 1, \forall t = 1, \dots, T, \\ -\infty & \text{otherwise.} \end{cases}$$

Consider a multi-dimensional generalized assignment problem featuring m bins, each with d' resources in quantity $b_{ij'}$. This problem is a special case of the packing problem, where $d = d' \cdot m$. Specifically, the packing problem creates one resource for each bin and each corresponding resource in the generalized assignment problem. The decision in the generalized assignment problem is $x^t = e_i$ if item t is assigned to bin i . The corresponding reward is C_i^t . The corresponding resource utilization A_{ij}^t is equal to 0 for each resource j associated with a bin i such that $x^t \neq e_i$ (i.e., in the generalized assignment problem, assigning an item to a bin only consumes resources from that bin). Therefore, consider a bin i_0 in the generalized assignment problem and a resource $j' \in \{1, \dots, d'\}$, where the (i_0, j') combination corresponds to resource $j \in \{1, \dots, d\}$ in the packing problem. The packing constraint $\sum_{t=1}^T \sum_{i=1}^m A_{ij}^t x_i^t \leq b_j$ becomes $\sum_{t=1}^T A_{i_0 j}^t x_{i_0}^t \leq b_j$, that is, $\sum_{t=1}^T A_{i_0 j}^t x_{i_0}^t \leq b_{i_0 j'}$, which retrieves the constraint from the generalized assignment formulation in Section 5.2.

Note that we formulate the problem as a maximization problem for simplicity and consistency with the packing literature, but this is obviously without loss of generality. The offline optimum OPT can be derived from the following integer optimization formulation:

$$\max \quad \sum_{t=1}^T \sum_{i=1}^m C_i^t x_i^t \quad (\text{EC.1})$$

$$\text{s.t.} \quad \sum_{t=1}^T \sum_{i=1}^m A_{ij}^t x_i^t \leq b_j, \quad \forall j = 1, \dots, d \quad (\text{EC.2})$$

$$x^t \in \Delta_I, \quad \forall t = 1, \dots, T \quad (\text{EC.3})$$

We use $a \cdot b$ to refer to the inner product of two m -dimensional vectors. For notational convenience, we also use $a \cdot b$ to refer to the column-wise inner product of an $m \times d$ matrix and an m -dimensional vector. We can thus re-write the problem as follows:

$$\text{OPT} = \max \left\{ \sum_{t=1}^T C^t \cdot x^t : \sum_{t=1}^T A^t \cdot x^t \leq b; x^t \in \Delta_I, \forall t = 1, \dots, T \right\} \quad (\text{EC.4})$$

The SSOA algorithm for the packing problem is given in Algorithm 3. Specifically, we denote by \tilde{C}_τ^t and \tilde{A}_τ^t the realizations sampled at time t for period $\tau > t$.

To formally state our guarantees, we need the definition of an *equivariant* solver.

DEFINITION EC.2. A solver is *equivariant* if, when we permute the items, the solution is permuted in the same way: if it returns (x^1, x^2, \dots, x^T) for $\max \left\{ \sum_{t=1}^T C^t \cdot x^t : \sum_{t=1}^T A^t \cdot x^t \leq b; x^t \in \Delta_I, \forall t = 1, \dots, T \right\}$, then for any permutation π of $\{1, \dots, T\}$ it returns $(x^{\pi(1)}, x^{\pi(2)}, \dots, x^{\pi(T)})$ for $\max \left\{ \sum_{t=1}^T C^{\pi(t)} \cdot x^{\pi(t)} : \sum_{t=1}^T A^{\pi(t)} \cdot x^{\pi(t)} \leq b; x^t \in \Delta_I, \forall t = 1, \dots, T \right\}$.

Any solver can be made equivariant by sorting items according to a pre-specified order (e.g., such that the uplets (C^t, A^t) are in lexicographic order) and applying the inverse permutation.

Algorithm 3 SSOA algorithm for the stochastic packing problem.

for $t = 1, \dots, T$ **do**

Observe the cost vector C^t and the resource requirements matrix A^t .

Sample \tilde{C}_τ^t and \tilde{A}_τ^t , for $\tau = t+1, \dots, T$ independently from distribution μ .

Given implemented decisions $(\bar{x}^1, \dots, \bar{x}^{t-1})$, find an optimal solution $(\bar{x}^t, \tilde{x}^{t+1}, \dots, \tilde{x}^T)$ for

$$\max_{x^t, \dots, x^T \in \Delta_I} \left\{ C^t \cdot x^t + \sum_{\tau=t+1}^T \tilde{C}_\tau^t \cdot x^\tau : \sum_{\sigma=1}^{t-1} A^\sigma \cdot \bar{x}^\sigma + A^t \cdot x^t + \sum_{\tau=t+1}^T \tilde{A}_\tau^t \cdot x^\tau \leq b \right\}. \quad (\text{EC.5})$$

Implement decision \bar{x}^t for the t -th item.

end for

We now prove the following result for the online packing problem. This directly implies Theorem 1 via the transformation $d \leftarrow d \cdot m$ (as detailed above, the dimension in the packing problem refers to the overall number of resources whereas the dimension in the generalized assignment problem refers to the number of resources per bin).

Theorem 3 *SSOA returns a feasible solution to the online packing problem, i.e., $\sum_{t=1}^T A^t \bar{x}^t \leq b$ with probability 1. Moreover, suppose there is $\varepsilon \in (0, 0.001]$ such that $b_j \geq 1024 \cdot \log\left(\frac{2dT}{\varepsilon}\right) \cdot \frac{\log^3(1/\varepsilon)}{\varepsilon^2} A_{ij}^t$ for all i, j, t for every matrix A in the support of μ . Then the solution satisfies $\mathbb{E}\left(\sum_{t=1}^T C^t \cdot \bar{x}^t\right) \geq (1 - \varepsilon)\mathbb{E}(\text{OPT})$, as long as the procedure relies on an equivariant solver.*

EC.2.1. Proof of Theorem 3

We prove the result with a discrete distribution μ . The general case follows from standard approximation arguments. Also, by construction, SSOA always returns a feasible solution.

Without loss of generality, assume that $A_{ij}^t \in [0, 1]$ for all i, j, t and that $b_j = B$ for all j (this can be easily obtained by rescaling the rows). By assumption, $B \geq 1024 \cdot \log\left(\frac{2dT}{\varepsilon}\right) \cdot \frac{\log^3(1/\varepsilon)}{\varepsilon^2}$.

Let us perform the change of variables $\bar{\varepsilon} := \frac{\varepsilon}{8 \log^{1.5}(1/\varepsilon)}$. We note two properties:

$$2 \cdot \log\left(\frac{2dT}{\varepsilon}\right) \geq \log\left(\frac{2dT}{\bar{\varepsilon}}\right) \quad (\text{EC.6})$$

$$8\bar{\varepsilon} \log(2/\bar{\varepsilon}) \leq \varepsilon \quad (\text{EC.7})$$

Equation (EC.6) is equivalent to $2dT \geq \frac{\varepsilon^2}{\bar{\varepsilon}}$ and, by definition of $\bar{\varepsilon}$, it is therefore equivalent to $2dT \geq 8\varepsilon \log^{1.5}(1/\varepsilon)$. It can be easily verified that $8\varepsilon \log^{1.5}(1/\varepsilon) \leq 1$ for all $\varepsilon \leq 0.001$, which implies Equation (EC.6). By definition of $\bar{\varepsilon}$, Equation (EC.7) is equivalent to $\log(2/\bar{\varepsilon}) \leq \log^{1.5}(1/\varepsilon)$, i.e., $\log\left(\frac{16 \log^{1.5}(1/\varepsilon)}{\varepsilon}\right) \leq \log^{1.5}(1/\varepsilon)$, which holds for all $\varepsilon \leq 0.001$.

By definition of $\bar{\varepsilon}$, we have $B \geq 16 \cdot \log\left(\frac{2dT}{\varepsilon}\right) \cdot \frac{1}{\bar{\varepsilon}^2}$, hence, per Equation (EC.6), $B \geq 8 \cdot \log\left(\frac{2dT}{\bar{\varepsilon}}\right) \cdot \frac{1}{\bar{\varepsilon}^2}$.

Let $\text{OPT}(s, b')$ denote the optimal value of the subproblem with the first s items and a right-hand side capacity of $b' \in \mathbb{R}^d$. It is formulated via the following stochastic optimization problem:

$$\text{OPT}(s, b') = \max \left\{ \sum_{t=1}^s C^t \cdot x^t : \sum_{t=1}^s A^t \cdot x^t \leq b'; x^t \in \Delta_I, \forall t = 1, \dots, s \right\} \quad (\text{EC.8})$$

Note that $\text{OPT}(s, b')$ is a random variable and that $\text{OPT}(T, B\mathbf{1})$ is equal to the original problem (where $\mathbf{1}$ denotes the d -dimensional vector of ones). [Gupta and Molinaro \(2016\)](#) prove that $\text{OPT}(s, b')$ scales with the fraction of timesteps $\frac{s}{T}$ and with the smallest fraction of budget available $\min_j \frac{b'_j}{B}$ in the more restrictive case where A^t is a $d \times 1$ vector. We extend this result in [Lemma EC.1](#) in the case where A^t is a $d \times m$ matrix, namely $\mathbb{E}(\text{OPT}(s, b')) \approx \min \left\{ \frac{s}{T}, \min_j \frac{b'_j}{B} \right\} \cdot \mathbb{E}(\text{OPT})$.

LEMMA EC.1. *Let $\zeta = \min \left\{ \frac{s}{T}, \min_j \frac{b'_j}{B} \right\}$. If $s \geq \bar{\varepsilon}^2 T$ and $\min_j b'_j \geq \bar{\varepsilon}^2 B$, then*

$$\mathbb{E}(\text{OPT}(s, b')) \geq \left[\zeta \left(1 - \bar{\varepsilon} \sqrt{\frac{1}{\zeta}} \right) - \frac{1 + \bar{\varepsilon}}{T} \right] \mathbb{E}(\text{OPT})$$

Proof. Again, without loss of generality, we assume that all coordinates of b' are identical, so $b' = B'\mathbf{1}$ and $B' = \min_j b'_j$, and that $\frac{B'}{B} = \min_j \frac{b'_j}{B} \leq \frac{s}{T}$. Otherwise, the condition is obtained by rescaling the rows.

Let x_* be an optimal solution to the original problem (hence, a solution that achieves $\text{OPT}(T, B\mathbf{1})$) returned by an equivariant solver. Also, let Set be the set of the data $\{(C^1, A^1), \dots, (C^T, A^T)\}$ of the problem. The definition of Set ignores the order, so conditioning on Set leaves the order of $\{(C^1, A^1), \dots, (C^T, A^T)\}$ uniformly random; in particular, conditioned on Set , the sequence of random variables C^1, \dots, C^T is exchangeable, so the distribution of the vector $(C^{\pi(1)}, \dots, C^{\pi(T)})$ is the same for every permutation π of $\{1, \dots, T\}$. Due to the equivariance of the solution x_* , the distribution of $C^t \cdot x_*^t$ is the same for all $t = 1, \dots, T$, conditioned on Set ; in particular, at time t , the contribution to the optimal solution is

$$\mathbb{E}[C^t \cdot x_*^t | Set] = \frac{1}{T} \cdot \mathbb{E} \left[\sum_{t=1}^T C^t \cdot x_*^t \mid Set \right] = \frac{\mathbb{E}[\text{OPT} | Set]}{T}. \quad (\text{EC.9})$$

Informally, the proof of the lemma relies on the observation that, for \tilde{s} slightly smaller than ζT , the solution truncated to its first \tilde{s} elements is a feasible solution with high probability to the problem given in Equation (EC.8), and yields an expected value $\tilde{s} \frac{\mathbb{E}(\text{OPT})}{T} \approx \zeta \mathbb{E}(\text{OPT})$. This will give that $\text{OPT}(s, b')$ is larger than but close to $\zeta \mathbb{E}(\text{OPT})$. Let us formalize these arguments.

Let $\tilde{B} := B' \left(1 - \bar{\varepsilon} \sqrt{B/B'} \right)$, and fix \tilde{s} to the integer in the interval $\left(\frac{T\tilde{B}}{B} - 1, \frac{T\tilde{B}}{B} \right]$. In particular, since $\tilde{B} \leq B' \leq \frac{sB}{T}$, we have that $\tilde{s} \leq s$. We first show that the solution $\hat{x} := (x_*^1, \dots, x_*^{\tilde{s}}, 0, \dots, 0) \in \mathbb{R}^s$ is feasible with high probability for Equation (EC.8). Again, conditioned on Set , the sequence of random variables A^1, \dots, A^T is exchangeable. Due to the equivariance of x_* , it follows that the

sequence of random variables $A_j^1 \cdot x_\star^1, \dots, A_j^T \cdot x_\star^T$ is also exchangeable. From the feasibility of x_\star , $\sum_{t=1}^T A_j^t \cdot x_\star^t \leq B$ in every scenario. From the concentration inequality for exchangeable sequences (Corollary 1 in EC.2.2), we obtain the following inequality (using $\tau = \bar{\varepsilon}\sqrt{BB'}$ and $M = B$):

$$\begin{aligned} \Pr\left(\sum_{t=1}^T A_j^t \cdot \hat{x}_j^t \geq B' \mid Set\right) &= \Pr\left(\sum_{t=1}^T A_j^t \cdot \hat{x}_j^t \geq \tilde{B} + \bar{\varepsilon}\sqrt{BB'} \mid Set\right) \\ &\leq \Pr\left(\sum_{t=1}^T A_j^t \cdot \hat{x}_j^t \geq \frac{\tilde{s}B}{T} + \bar{\varepsilon}\sqrt{BB'} \mid Set\right) \\ &\leq 2 \exp\left(-\min\left\{\frac{\bar{\varepsilon}^2 B'T}{8\tilde{s}}, \frac{\bar{\varepsilon}\sqrt{BB'}}{2}\right\}\right). \end{aligned} \quad (\text{EC.10})$$

To upper bound the right-hand side, we use $B \geq \frac{8}{\bar{\varepsilon}^2} \log\left(\frac{2dT}{\bar{\varepsilon}}\right)$, $\tilde{B} \leq B'$ and $\tilde{s} \leq \frac{T\tilde{B}}{B}$ to obtain:

$$\frac{\bar{\varepsilon}^2 B'T}{8\tilde{s}} \geq \frac{\bar{\varepsilon}^2 B'B}{8\tilde{B}} \geq \frac{\bar{\varepsilon}^2 B}{8} \geq \log\left(\frac{2dT}{\bar{\varepsilon}}\right).$$

Moreover, the assumption that $B' \geq \bar{\varepsilon}^2 B$ implies:

$$\frac{\bar{\varepsilon}\sqrt{BB'}}{2} \geq \frac{\bar{\varepsilon}^2 B}{2} \geq 4 \log\left(\frac{2dT}{\bar{\varepsilon}}\right).$$

Thus, the solution violates the j -th constraint of (IP(s, b')) with probability at most $\frac{\bar{\varepsilon}}{dT}$:

$$\Pr\left(\sum_{t=1}^T A_j^t \cdot \hat{x}_j^t \geq B' \mid Set\right) \leq \frac{\bar{\varepsilon}}{dT}.$$

Taking a union bound over all d constraints, the solution is feasible with probability at least $1 - \frac{\bar{\varepsilon}}{T}$:

$$\Pr\left(\sum_{t=1}^T A^t \cdot \hat{x}^t \leq B'\mathbf{1} \mid Set\right) \geq 1 - \frac{\bar{\varepsilon}}{T}.$$

Let G be the good event that this feasibility condition holds (and G^c be its complement). Under this event, $\text{OPT}(s, b')$ is at least equal to $\sum_{t=1}^{\tilde{s}} C^t \cdot \hat{x}^t$. We obtain:

$$\begin{aligned} \mathbb{E}\left[\text{OPT}(s, b') \mid Set\right] &\geq \mathbb{E}\left[\sum_{t=1}^{\tilde{s}} C^t \cdot \hat{x}^t \mid G \text{ and } Set\right] \cdot \Pr(G \mid Set) \\ &= \mathbb{E}\left[\sum_{t=1}^{\tilde{s}} C^t \cdot \hat{x}^t \mid Set\right] - \mathbb{E}\left[\sum_{t=1}^{\tilde{s}} C^t \cdot \hat{x}^t \mid G^c \text{ and } Set\right] \cdot \Pr(G^c \mid Set) \\ &\geq \mathbb{E}\left[\sum_{t=1}^{\tilde{s}} C^t \cdot \hat{x}^t \mid Set\right] - \mathbb{E}\left[\text{OPT} \mid G^c \text{ and } Set\right] \cdot \Pr(G^c \mid Set), \end{aligned} \quad (\text{EC.11})$$

where the last inequality stems from the feasibility of \hat{x} in the full problem.

To bound the first term, recall that $C^t \cdot \hat{x}^t = C^t \cdot x_*^t$ for $t \leq \tilde{s}$, so Equation (EC.9) implies $\mathbb{E}[C^t \cdot \hat{x}^t \mid \text{Set}] = \frac{\mathbb{E}[\text{OPT} \mid \text{Set}]}{T}$. For the second term, notice that conditioning on Set fixes the items in the instance, hence the optimal value OPT , so further conditioning on G^c has no effect. Therefore:

$$\begin{aligned} \mathbb{E} \left[\text{OPT}(s, b') \mid \text{Set} \right] &\geq \frac{\tilde{s}}{T} \mathbb{E}[\text{OPT} \mid \text{Set}] - \frac{\bar{\varepsilon}}{T} \mathbb{E}[\text{OPT} \mid \text{Set}] \\ &\geq \left[\frac{\tilde{B}}{B} - \frac{1}{T} - \frac{\bar{\varepsilon}}{T} \right] \cdot \mathbb{E}[\text{OPT} \mid \text{Set}] \\ &= \left[\frac{B'}{B} \left(1 - \bar{\varepsilon} \sqrt{\frac{B}{B'}} \right) - \frac{1 + \bar{\varepsilon}}{T} \right] \cdot \mathbb{E}[\text{OPT} \mid \text{Set}] \\ &\geq \left[\zeta \left(1 - \bar{\varepsilon} \sqrt{\frac{1}{\zeta}} \right) - \frac{1 + \bar{\varepsilon}}{T} \right] \cdot \mathbb{E}[\text{OPT} \mid \text{Set}], \end{aligned}$$

where the last inequality uses that, by assumption, $\zeta \geq \bar{\varepsilon}^2$, and the function $x \mapsto x(1 - \bar{\varepsilon} \sqrt{1/x})$ is increasing for $x \geq \bar{\varepsilon}^2$. Taking expectation with respect to Set concludes the proof of the lemma. \square

Now let $S_t := A^1 \cdot \bar{x}_1 + \dots + A^t \cdot \bar{x}^t$ be the occupation vector at time t ($S_0 = 0$ by convention). We show that by time t , the algorithm utilizes approximately a fraction $\frac{t}{T}$ of the overall budget, i.e., S_t is less than but close to $\frac{t}{T} B \mathbf{1}$. In fact, we prove a stronger result, which will be used to show that S_t is concentrated around its mean. Let \mathcal{F}_t denote the σ -algebra generated by the history up to time t , i.e., the data $(C^1, A^1), \dots, (C^t, A^t)$ and the samples $\tilde{C}_\tau^{t'}$ and matrices $\tilde{A}_\tau^{t'}$, for $t' = 1, \dots, t$ and $\tau = t' + 1, \dots, T$. Let \mathbb{E}_t denote the expectation conditioned on the history \mathcal{F}_t . We can now prove the following result:

LEMMA EC.2. *For every $t \geq 1$, we have*

$$\mathbb{E}_{t-1} S_t \leq \left(1 - \frac{1}{T-t+1} \right) S_{t-1} + \frac{B \mathbf{1}}{T-t+1}. \quad (\text{EC.12})$$

In particular, $\mathbb{E} S_t \leq \frac{t}{T} B \mathbf{1}$.

Proof. Fix a time t . By construction, the algorithm yields a feasible solution to the problem, that is:

$$S_{t-1} + A^t \cdot \bar{x}^t + \tilde{A}_{t+1}^t \cdot \tilde{x}^{t+1} + \dots + \tilde{A}_T^t \cdot \tilde{x}_T \leq B \mathbf{1}. \quad (\text{EC.13})$$

Note that, even conditioned on the history up to time $t-1$, the matrices $A^t, \tilde{A}_{t+1}^t, \dots, \tilde{A}_T^t$ are sampled i.i.d. and the solution $\bar{x}^t, \tilde{x}^{t+1}, \dots, \tilde{x}_T$ is by assumption equivariant. Therefore, conditioned on the history up to time $t-1$, the sequence of vectors $A^t \cdot \bar{x}^t, \tilde{A}_{t+1}^t \cdot \tilde{x}^{t+1}, \dots, \tilde{A}_T^t \cdot \tilde{x}_T$ is again an exchangeable sequence of random variables. In particular, $\mathbb{E}_{t-1}(A^t \cdot \bar{x}^t) = \mathbb{E}_{t-1}(\tilde{A}_\tau^t \cdot \tilde{x}_\tau)$ for all $\tau > t$. From Equation (EC.13), it comes:

$$S_{t-1} + (T-t+1) \mathbb{E}_{t-1}(A^t \cdot \bar{x}^t) \leq B \mathbf{1}.$$

We obtain inequality (EC.12):

$$\begin{aligned}\mathbb{E}_{t-1}S_t &= S_{t-1} + \mathbb{E}_{t-1}(A^t \cdot \bar{x}^t) \\ &\leq S_{t-1} + \frac{B\mathbf{1} - S_{t-1}}{T-t+1} \\ &= \left(1 - \frac{1}{T-t+1}\right) S_{t-1} + \frac{B\mathbf{1}}{T-t+1}.\end{aligned}$$

We now prove that $\mathbb{E}S_t \leq \frac{t}{T}B\mathbf{1}$ by induction on t . It clearly holds for $t=0$. Assuming that it holds for $t-1$, we obtain:

$$\begin{aligned}\mathbb{E}S_t &= \mathbb{E}(\mathbb{E}_{t-1}S_t) \leq \left(1 - \frac{1}{T-t+1}\right) \mathbb{E}(S_{t-1}) + \frac{B\mathbf{1}}{T-t+1} \\ &\leq \left(1 - \frac{1}{T-t+1}\right) \frac{t-1}{T} \cdot B\mathbf{1} + \frac{B\mathbf{1}}{T-t+1} \\ &= \frac{t}{T}B\mathbf{1},\end{aligned}$$

where the first inequality follows from inequality (EC.12) and the next inequality follows by the induction hypothesis. This concludes the proof. \square

While this lemma guarantees that the occupation vector $\mathbb{E}(S_t)$ is at most $\frac{t}{T}B\mathbf{1}$ in expectation, we need high-probability guarantees. We derive them in the next lemma.

LEMMA EC.3. *For each $t \geq \frac{\bar{\varepsilon}^2 T}{4}$, we have:*

$$\Pr\left(S_t \leq \left(1 + \bar{\varepsilon}\sqrt{\frac{T}{t}}\right) \frac{t}{T}B\mathbf{1}\right) \geq 1 - \frac{\bar{\varepsilon}}{2T}.$$

Proof. We show that for every component $j = 1, \dots, d$, $(S_t)_j$ is concentrated around its expected value, namely that $(S_t)_j \leq \left(1 + \bar{\varepsilon}\sqrt{\frac{T}{t}}\right) \frac{t}{T}B$ with probability at least $1 - \frac{\bar{\varepsilon}}{2T}$. But since the increments $A^1 \cdot \bar{x}^1, \dots, A^t \cdot \bar{x}^t$ are not independent (e.g., \bar{x}^t depends on A^1, \dots, A^t), we cannot use standard concentration inequalities. Instead, we rely on a concentration result for “self-centering” sequences, given in Theorem 5 (see EC.2.2 for the appropriate definitions).

Let us denote $\alpha_t := 1 - \frac{1}{T-t+1}$ and $\beta_t := \frac{B}{T-t+1}$ the constants in Lemma EC.2, and let μ_t be the solution to the recurrence relation $y_t = \alpha_t y_{t-1} + \beta_t$ and $y_0 = 0$. From Theorem 5, we obtain, for any $\gamma \in (0, 1]$:

$$\Pr((S_t)_j \geq (1 + 2\gamma)\mu_t) \leq e^{-\gamma^2 \mu_t}. \quad (\text{EC.14})$$

By proceeding as in the proof of Lemma EC.2, we prove by induction on t that $\mu_t = \frac{t}{T}B$: this is clearly true for $t=0$, and then we obtain:

$$\mu_t = \left(1 - \frac{1}{T-t+1}\right) \mu_{t-1} + \frac{B}{T-t+1} = \left(1 - \frac{1}{T-t+1}\right) \frac{t-1}{T}B + \frac{B}{T-t+1} = \frac{t}{T}B.$$

From Equation (EC.14) with $\gamma = \frac{\bar{\varepsilon}}{2}\sqrt{T/t}$ ($\gamma \leq 1$ by assumption), we derive:

$$\Pr \left((S_t)_j \geq \left(1 + \bar{\varepsilon} \sqrt{\frac{T}{t}} \right) \frac{t}{T} B \right) \leq e^{-\frac{\bar{\varepsilon}^2}{4} B}.$$

Recall that, by assumption, $B \geq \frac{8}{\bar{\varepsilon}^2} \log \left(\frac{2dT}{\bar{\varepsilon}} \right) \geq \frac{4}{\bar{\varepsilon}^2} \log \left(\frac{2dT}{\bar{\varepsilon}} \right)$. This yields:

$$\Pr \left((S_t)_j \geq \left(1 + \bar{\varepsilon} \sqrt{\frac{T}{t}} \right) \frac{t}{T} B \right) \leq e^{-\log(2dT/\bar{\varepsilon})} = \frac{\bar{\varepsilon}}{2dT}.$$

Taking a union bound over all d coordinates, we obtain:

$$\Pr \left(S_t \leq \left(1 + \bar{\varepsilon} \sqrt{\frac{T}{t}} \right) \frac{t}{T} B \mathbf{1} \right) \geq 1 - \frac{\bar{\varepsilon}}{2T}.$$

This concludes the proof of the lemma. \square

We now lower bound $C^t \cdot \bar{x}^t$ obtained by the algorithm at time t . From Lemma EC.3, there is about $(1 - \frac{t-1}{T})B$ of the budget left in each of the constraints, and so the remaining value should be $(1 - \frac{t-1}{T})\mathbb{E}(\text{OPT})$. Moreover, since there are $T - t + 1$ variables in the remaining problem, we expect that \bar{x}^t accrues a value of $\frac{1}{T-t+1} (1 - \frac{t-1}{T})\mathbb{E}(\text{OPT})$, or $\frac{1}{T}\mathbb{E}(\text{OPT})$. This is formalized below.

LEMMA EC.4. *For every t satisfying $\bar{\varepsilon}^2 T \leq t \leq (1 - 2\bar{\varepsilon})T$ we have:*

$$\mathbb{E}(C^t \cdot \bar{x}^t) \geq \left[1 - \bar{\varepsilon} \sqrt{\frac{T}{(1-\bar{\varepsilon})T-t}} - 2\bar{\varepsilon} \frac{\sqrt{Tt}}{T-t} - \frac{1+\bar{\varepsilon}}{T-t+1} \right] \frac{\mathbb{E}(\text{OPT})}{T}.$$

Proof. Fix t such that $\bar{\varepsilon}^2 T \leq t \leq T(1 - 2\bar{\varepsilon})$, and consider the solution $\bar{x}^t, \tilde{x}^{t+1}, \dots, \tilde{x}^T$ obtained by the algorithm at this time. By definition, we have:

$$C^t \cdot \bar{x}^t + \tilde{C}_{t+1}^t \cdot \tilde{x}^{t+1} + \dots + \tilde{C}_T^t \cdot \tilde{x}^T = \max_{x^t, \dots, x^T \in \Delta_I} \left\{ C^t \cdot x^t + \sum_{\tau=t+1}^T \tilde{C}_\tau^t \cdot x^\tau : A^t \cdot x^t + \sum_{\tau=t+1}^T \tilde{A}_\tau^t \cdot x^\tau \leq B\mathbf{1} - S_{t-1} \right\}.$$

Conditioning on the history \mathcal{F}_{t-1} fixes the occupation vector S_{t-1} , hence the right-hand side of the resource constraint. The expected value of the stochastic program is equal to $\mathbb{E}(\text{OPT}(T-t+1, B\mathbf{1} - S_{t-1}))$. It comes:

$$\mathbb{E}_{t-1} \left[C^t \cdot \bar{x}^t + \tilde{C}_{t+1}^t \cdot \tilde{x}^{t+1} + \dots + \tilde{C}_T^t \cdot \tilde{x}^T \right] = \mathbb{E}(\text{OPT}(T-t+1, B\mathbf{1} - S_{t-1})). \quad (\text{EC.15})$$

As earlier, conditioned on \mathcal{F}_{t-1} the random variables $C^t \cdot \bar{x}^t, \tilde{C}_{t+1}^t \cdot \tilde{x}^{t+1}, \dots, \tilde{C}_T^t \cdot \tilde{x}^T$ form an exchangeable sequence and thus have the same conditional expectations. Thus, all the terms on the left-hand side of Equation (EC.15) have the same expectation. In particular,

$$\mathbb{E}_{t-1}(C^t \cdot \bar{x}^t) = \frac{1}{T-t+1} \cdot \mathbb{E}(\text{OPT}(T-t+1, B\mathbf{1} - S_{t-1})).$$

Now, let $\gamma_t := \bar{\varepsilon} \sqrt{\frac{T}{t}}$. From Lemma EC.3, we know that, with probability at least $1 - \frac{\bar{\varepsilon}}{2T}$, we have $S_{t-1} \leq (1 + \gamma_{t-1}) \frac{t-1}{T} B\mathbf{1}$, hence $B\mathbf{1} - S_{t-1} \geq (1 - (1 + \gamma_{t-1}) \frac{t-1}{T}) B\mathbf{1}$. When this event, called G , transpires, we have from Lemma EC.1, with $\zeta_t := \min \left\{ \frac{T-t+1}{T}, 1 - (1 + \gamma_{t-1}) \frac{t-1}{T} \right\} = 1 - (1 + \gamma_{t-1}) \frac{t-1}{T}$

$$\mathbb{E}(\text{OPT}(T-t+1, B\mathbf{1} - S_{t-1})) \geq \left[\zeta_t \left(1 - \bar{\varepsilon} \sqrt{\frac{1}{\zeta_t}} \right) - \frac{1 + \bar{\varepsilon}}{T} \right] \cdot \mathbb{E}(\text{OPT}).$$

Note that the assumptions in Lemma EC.1 are met because $t \leq (1 - 2\bar{\varepsilon})T$ and $\bar{\varepsilon} \in (0, 1]$. Then:

$$\begin{aligned} \mathbb{E}(C^t \cdot \bar{x}^t) &\geq \mathbb{E}(C^t \cdot \bar{x}^t \mid G) \cdot \Pr(G) \\ &\geq \left(1 - \frac{\bar{\varepsilon}}{2T} \right) \left[\zeta_t \left(1 - \bar{\varepsilon} \sqrt{\frac{1}{\zeta_t}} \right) - \frac{1 + \bar{\varepsilon}}{T} \right] \frac{\mathbb{E}(\text{OPT})}{T-t+1} \\ &\geq \left[\left(1 - \frac{\bar{\varepsilon}}{T} \right) \left(1 - \bar{\varepsilon} \sqrt{\frac{1}{\zeta_t}} \right) \frac{\zeta_t}{T-t+1} - \frac{1 + \bar{\varepsilon}}{T(T-t+1)} \right] \mathbb{E}(\text{OPT}). \end{aligned} \quad (\text{EC.16})$$

To further lower bound the right-hand side, using the definitions of ζ_t and γ_{t-1} we have

$$\begin{aligned} \frac{\zeta_t}{T-t+1} &= \frac{(T-t+1) - \gamma_{t-1}(t-1)}{T(T-t+1)} \\ &= \frac{1}{T} \left(1 - \bar{\varepsilon} \frac{\sqrt{T}\sqrt{t-1}}{T-t+1} \right) \\ &\geq \frac{1}{T} \left(1 - \bar{\varepsilon} \frac{\sqrt{T}\sqrt{t}}{T-t} \right) \end{aligned}$$

Replacing in Equation (EC.16) and using that $(1-a)(1-b) \geq 1-a-b$ for $a, b \geq 0$, we obtain:

$$\begin{aligned} \mathbb{E}(C^t \cdot \bar{x}^t) &\geq \left[\left(1 - \frac{\bar{\varepsilon}}{T} \right) \left(1 - \bar{\varepsilon} \sqrt{\frac{1}{\zeta_t}} \right) \left(1 - \bar{\varepsilon} \frac{\sqrt{T}\sqrt{t}}{T-t} \right) - \frac{1 + \bar{\varepsilon}}{T-t+1} \right] \frac{\mathbb{E}(\text{OPT})}{T} \\ &\geq \left[1 - \frac{\bar{\varepsilon}}{T} - \bar{\varepsilon} \sqrt{\frac{1}{\zeta_t}} - \bar{\varepsilon} \frac{\sqrt{T}\sqrt{t}}{T-t} - \frac{1 + \bar{\varepsilon}}{T-t+1} \right] \frac{\mathbb{E}(\text{OPT})}{T} \\ &\geq \left[1 - \bar{\varepsilon} \sqrt{\frac{1}{\zeta_t}} - 2\bar{\varepsilon} \frac{\sqrt{T}\sqrt{t}}{T-t} - \frac{1 + \bar{\varepsilon}}{T-t+1} \right] \frac{\mathbb{E}(\text{OPT})}{T}. \end{aligned}$$

We can complete the lower bound of this right-hand side using

$$\zeta_t = \frac{(T-t+1)}{T} - \bar{\varepsilon} \sqrt{\frac{t-1}{T}} \geq \frac{(1-\bar{\varepsilon})T-t}{T}$$

We obtain:

$$\mathbb{E}(C^t \cdot \bar{x}^t) \geq \left[1 - \bar{\varepsilon} \sqrt{\frac{T}{(1-\bar{\varepsilon})T-t}} - 2\bar{\varepsilon} \frac{\sqrt{T}\sqrt{t}}{T-t} - \frac{1 + \bar{\varepsilon}}{T-t+1} \right] \frac{\mathbb{E}(\text{OPT})}{T}.$$

This concludes the proof of the lemma. \square

We are now ready to prove the guarantee of the SSOA algorithm stated in Theorem 3.

Proof of Theorem 3. Let ALG be the value achieved by the SSOA algorithm. From Lemma EC.4, we have:

$$\mathbb{E}(\text{ALG}) \geq \sum_{t=\bar{\varepsilon}^2 T}^{(1-2\bar{\varepsilon})T-1} \left(1 - \bar{\varepsilon} \sqrt{\frac{T}{(1-\bar{\varepsilon})T-t}} - 2\bar{\varepsilon} \frac{\sqrt{T}\sqrt{t}}{T-t} - \frac{1+\bar{\varepsilon}}{T-t+1} \right) \frac{\mathbb{E}(\text{OPT})}{T}. \quad (\text{EC.17})$$

Since the function $\sqrt{\frac{T}{(1-\bar{\varepsilon})T-t}}$ is increasing in t , we can use an integral to upper bound the sum:

$$\begin{aligned} \sum_{t=\bar{\varepsilon}^2 T}^{(1-2\bar{\varepsilon})T-1} \sqrt{\frac{T}{(1-\bar{\varepsilon})T-t}} &\leq \int_0^{(1-2\bar{\varepsilon})T} \sqrt{\frac{T}{(1-\bar{\varepsilon})T-t}} dt \\ &= \sqrt{T} \int_{\bar{\varepsilon}T}^{(1-\bar{\varepsilon})T} \frac{1}{\sqrt{y}} dy \\ &= 2\sqrt{T} \left(\sqrt{(1-\bar{\varepsilon})T} - \sqrt{\bar{\varepsilon}T} \right) \\ &\leq 2T. \end{aligned}$$

Similarly, since the function $\frac{\sqrt{t}}{T-t}$ is increasing in t , we have:

$$\begin{aligned} \sum_{t=\bar{\varepsilon}^2 T}^{(1-2\bar{\varepsilon})T-1} \frac{\sqrt{T}\sqrt{t}}{T-t} &= \sum_{t=\bar{\varepsilon}^2 T}^{(1-2\bar{\varepsilon})T-1} \frac{\sqrt{t/T}}{1-(t/T)} \\ &\leq \int_0^{(1-2\bar{\varepsilon})T} \frac{\sqrt{t/T}}{1-t/T} dt \\ &= T \int_0^{1-2\bar{\varepsilon}} \frac{\sqrt{y}}{1-y} dy. \end{aligned}$$

Therefore,

$$\begin{aligned} \sum_{t=\bar{\varepsilon}^2 T}^{(1-2\bar{\varepsilon})T-1} \frac{\sqrt{T}\sqrt{t}}{T-t} &\leq T \cdot \left[-2\sqrt{y} + \log \left(\frac{1+\sqrt{y}}{1-\sqrt{y}} \right) \right] \Big|_0^{1-2\bar{\varepsilon}} \\ &\leq T \log \left(\frac{1+\sqrt{1-2\bar{\varepsilon}}}{1-\sqrt{1-2\bar{\varepsilon}}} \right) \\ &\leq T \log \left(\frac{2}{1-\sqrt{1-2\bar{\varepsilon}}} \right) \\ &\leq T \log(2/\bar{\varepsilon}), \end{aligned}$$

where the last inequality uses the fact that $\sqrt{1+x} \leq 1 + \frac{x}{2}$ for all $x \in [-1, \infty)$.

Finally, the third negative term can be bounded as

$$\begin{aligned} \sum_{t=\bar{\varepsilon}^2 T}^{(1-2\bar{\varepsilon})T-1} \frac{1+\bar{\varepsilon}}{T-t+1} &\leq \int_{\bar{\varepsilon}^2 T}^{(1-2\bar{\varepsilon})T} \frac{1+\bar{\varepsilon}}{T-t+1} dt \\ &= \int_{1+2\bar{\varepsilon}T}^{1+(1-\bar{\varepsilon}^2)T} \frac{1+\bar{\varepsilon}}{y} dy \\ &= (1+\bar{\varepsilon}) \log(y) \Big|_{1+2\bar{\varepsilon}T}^{1+(1-\bar{\varepsilon}^2)T} \\ &\leq (1+\bar{\varepsilon}) \log(1/\bar{\varepsilon}) \end{aligned}$$

Combining these bounds into Equation (EC.17), we conclude:

$$\begin{aligned}\mathbb{E}(\text{ALG}) &\geq \left(1 - 2\bar{\varepsilon} - 2\bar{\varepsilon} \log(2/\bar{\varepsilon}) - \frac{1 + \bar{\varepsilon}}{T} \log(1/\bar{\varepsilon})\right) \mathbb{E}(\text{OPT}) \\ &\geq (1 - 8\bar{\varepsilon} \log(2/\bar{\varepsilon})) \mathbb{E}(\text{OPT}) \\ &\geq (1 - \varepsilon) \mathbb{E}(\text{OPT}).\end{aligned}$$

The second inequality uses the assumption that $T \geq \frac{1}{\bar{\varepsilon}}$ (otherwise, the facts that $B \geq \frac{1}{\bar{\varepsilon}}$ and the matrices A^t have entries in $[0, 1]$ make all constraints redundant and the problem becomes trivial).

The third inequality comes from Equation (EC.7). This concludes the proof of Theorem 3.

EC.2.2. Concentration Inequalities

Our analysis uses concentration inequalities for stochastic processes with dependent increments.

EC.2.2.1. Concentration inequality for exchangeable sequences.

Recall Bernstein's inequality for sampling without replacement.

Theorem 4 (Theorem 2.14.19 in Van Der Vaart and Wellner (1996)) *Let $A = \{a_1, \dots, a_n\}$ be a set of real numbers in the interval $[0, 1]$. Let S be a random subset of A of size s and let $A_S = \sum_{i \in S} a_i$. Setting $\mu = \frac{1}{n} \sum_{i=1}^n a_i$ and $\sigma^2 = \frac{1}{n} \sum_{i=1}^n (a_i - \mu)^2$, we have that for every $\tau > 0$*

$$\Pr(|A_S - s\mu| \geq \tau) \leq 2 \exp\left(-\frac{\tau^2}{2s\sigma^2 + \tau}\right).$$

A sequence X_1, \dots, X_n of random variables is *exchangeable* if its distribution is permutation invariant, i.e., the distribution of the vector $(X_{\pi(1)}, X_{\pi(2)}, \dots, X_{\pi(n)})$ is the same for all permutations π of $\{1, \dots, n\}$. The following result is the main result of this section.

Corollary 1 *Let X_1, \dots, X_n be an exchangeable sequence of random variables in the interval $[0, 1]$. Assume that $\sum_{i=1}^n X_i \leq M$ with probability 1. Then for every $s \in \{1, \dots, n\}$ and $\tau > 0$, we have*

$$\Pr\left(X_1 + \dots + X_s \geq \frac{sM}{n} + \tau\right) \leq 2 \exp\left(-\min\left\{\frac{\tau^2 n}{8sM}, \frac{\tau}{2}\right\}\right).$$

Proof. We prove the result in the case where the distribution μ is discrete. The general case following from standard approximation arguments.

Consider a set $A = \{a_1, \dots, a_n\}$ of n values in $[0, 1]$, and define $\mu := \frac{1}{n} \sum_{i=1}^n a_i$ and $\sigma^2 := \frac{1}{n} \sum_{i=1}^n (a_i - \mu)^2$. Condition on the set $\{X_1, \dots, X_n\}$ being equal to A , leaving their *order* free. Under this conditioning, X_1, \dots, X_s is just a random subset of size s from A , and $\mu = \frac{1}{n} \sum_{i=1}^n X_i \leq \frac{M}{n}$.

From Theorem 4, we get

$$\Pr\left(X_1 + \dots + X_s \geq \frac{sM}{n} + \tau \mid \{X_1, \dots, X_n\} = A\right) \leq 2 \exp\left(-\frac{\tau^2}{2s\sigma^2 + \tau}\right). \quad (\text{EC.18})$$

Since the a_i 's belong to the interval $[0, 1]$, the variance term can be bounded as

$$\sigma^2 = \frac{1}{n} \sum_{i=1}^n (a_i - \mu)^2 \leq \frac{1}{n} \sum_{i=1}^n |a_i - \mu| \leq \frac{1}{n} \left(\sum_{i=1}^n |a_i| + \sum_{i=1}^n |\mu| \right) = 2\mu \leq \frac{2M}{n}.$$

Further using the inequality $\frac{1}{a+b} \geq \frac{1}{2} \min\{\frac{1}{a}, \frac{1}{b}\}$ for non-negative a, b , we obtain:

$$\exp\left(-\frac{\tau^2}{2s\sigma^2 + \tau}\right) \leq \exp\left(-\frac{\tau^2}{4sM/n + \tau}\right) \leq \exp\left(-\frac{1}{2} \min\left\{\frac{\tau^2 n}{4sM}, \tau\right\}\right).$$

Taking the expectation of (EC.18) over all possible sets A completes the proof. \square

EC.2.2.2. Concentration for affine stochastic processes

Theorem 5 Consider a sequence X_1, \dots, X_T of (possibly dependent) random variables in $[0, 1]$ adapted to a filtration $\mathcal{F}_1, \dots, \mathcal{F}_T$. Define the partial sums $S_t = X_1 + \dots + X_t$ for $t \in \{0, 1, \dots, T\}$ (with $S_0 = 0$). Furthermore, suppose that there are sequences $\alpha_1, \dots, \alpha_T \in [0, 1]$ and $\beta_1, \dots, \beta_T \geq 0$ such that $\mathbb{E}[S_t | \mathcal{F}_{t-1}] \leq \alpha_t S_{t-1} + \beta_t$ for all t . Then for every $\gamma \in (0, 1]$, we have

$$\Pr(S_T \geq (1 + 2\gamma)\mu_T) \leq e^{-\gamma^2 \mu_T},$$

where μ_1, \dots, μ_T is the solution to the recursion $y_t = \alpha_t y_{t-1} + \beta_t$ (with $y_0 = 0$).

We make use of a lemma on the moment-generating function of affine transformations of S_t .

LEMMA EC.5. Consider a function $f(x) = ax + b$ with $a \in [0, 1]$. Under the assumptions from Theorem 5, for all $\gamma \in (0, 1]$ we have

$$\mathbb{E}(e^{\gamma f(S_t)}) \leq \mathbb{E}(e^{\gamma f(\alpha_t S_{t-1} + (1+\gamma)\beta_t)}).$$

Proof. Since conditioning on \mathcal{F}_{t-1} fixes the sum S_{t-1} , we observe that

$$\mathbb{E}(e^{\gamma f(S_t)}) = \mathbb{E}(e^{\gamma(aS_t + b)}) = \mathbb{E}\left[e^{\gamma(aS_{t-1} + b)} \mathbb{E}\left[e^{\gamma a X_t} \mid \mathcal{F}_{t-1}\right]\right]. \quad (\text{EC.19})$$

Using the inequality $e^x \leq 1 + x + x^2$ for $x \in [0, 1]$, and then the inequality $1 + x \leq e^x$, we get:

$$\mathbb{E}\left[e^{\gamma a X_t} \mid \mathcal{F}_{t-1}\right] \leq \mathbb{E}\left[1 + \gamma a X_t + \gamma^2 a^2 X_t^2 \mid \mathcal{F}_{t-1}\right] \quad (\text{EC.20})$$

$$\begin{aligned} &\leq \mathbb{E}\left[1 + (\gamma + \gamma^2) a X_t \mid \mathcal{F}_{t-1}\right] \\ &= 1 + (\gamma + \gamma^2) a \mathbb{E}[X_t | \mathcal{F}_{t-1}] \\ &\leq e^{(\gamma + \gamma^2) a \mathbb{E}[X_t | \mathcal{F}_{t-1}]}. \end{aligned} \quad (\text{EC.21})$$

Since $S_t = S_{t-1} + X_t$, the assumption $\mathbb{E}[S_t | \mathcal{F}_{t-1}] \leq \alpha_t S_{t-1} + \beta_t$ implies $\mathbb{E}[X_t | \mathcal{F}_{t-1}] \leq (\alpha_t - 1)S_{t-1} + \beta_t$. Applying this to Equation (EC.21), we obtain the following inequality, using the fact that $\gamma^2 a(\alpha_t - 1)S_t \leq 0$:

$$\mathbb{E}\left[e^{\gamma a X_t} \mid \mathcal{F}_{t-1}\right] \leq e^{(\gamma + \gamma^2) a ((\alpha_t - 1)S_{t-1} + \beta_t)} \leq e^{\gamma a ((\alpha_t - 1)S_{t-1} + \beta_t) + \gamma^2 a \beta_t}.$$

From Equation (EC.19), it comes:

$$\mathbb{E} \left(e^{\gamma f(S_t)} \right) \leq \mathbb{E} \left[e^{\gamma(a\alpha_t S_{t-1} + (1+\gamma)\beta_t + b)} \right] = \mathbb{E} \left[e^{\gamma f(\alpha_t S_{t-1} + (1+\gamma)\beta_t)} \right].$$

This concludes the proof of the lemma. \square

Proof of Theorem 5.

Define the affine function $f_t(x) := \alpha_t x + (1 + \gamma)\beta_t$, so that the previous lemma can be expressed as $\mathbb{E} \left(e^{\gamma f(S_t)} \right) \leq \mathbb{E} \left(e^{\gamma f(f_t(S_{t-1}))} \right)$. Applying this lemma repeatedly gives:

$$\mathbb{E} \left(e^{\gamma S_T} \right) \leq \mathbb{E} \left(e^{\gamma f_T(S_{T-1})} \right) \leq \mathbb{E} \left(e^{\gamma f_T(f_{T-1}(S_{T-2}))} \right) \leq \dots \leq \mathbb{E} \left(e^{\gamma f_T(f_{T-1}(\dots f_2(S_1)))} \right) \leq \mathbb{E} \left(e^{\gamma f_T(f_{T-1}(\dots f_2(f_1(0))))} \right).$$

We can still apply the previous lemma because the composed function $f_T \circ f_{T-1} \circ \dots \circ f_t$ is still affine of the form $a_t x + b_t$ with $a_t \in [0, 1]$ and $b_t \geq 0$ (indeed, $a = \alpha_T \dots \alpha_t \in [0, 1]$ and b is obtained by taking products and sums of the α_t 's and β_t 's, which are all non-negative).

Moreover, we prove by induction on $t = 1, \dots, T$ that the composition of these functions satisfies:

$$f_t(f_{t-1}(\dots f_2(f_1(0)))) = (1 + \gamma)\mu_t.$$

For $t = 0$, we have $f_1(0) = (1 + \gamma)\beta_1 = (1 + \gamma)\mu_1$. For $t \geq 1$, we have:

$$f_t(f_{t-1}(\dots f_2(f_1(0)))) = f_t((1 + \gamma)\mu_{t-1}) = (1 + \gamma) [\alpha_t \mu_{t-1} + \beta_t] = (1 + \gamma)\mu_t.$$

Thus, we get the moment-generating function upper bound $\mathbb{E} \left(e^{\gamma S_T} \right) \leq e^{\gamma(1+\gamma)\mu_T}$. Finally, applying Markov's inequality we get

$$\Pr(S_T \geq (1 + 2\gamma)\mu_T) = \Pr(e^{\gamma S_T} \geq e^{\gamma(1+2\gamma)\mu_T}) \leq \frac{\mathbb{E}(e^{\gamma S_T})}{e^{\gamma(1+2\gamma)\mu_T}} \leq \frac{e^{\gamma(1+\gamma)\mu_T}}{e^{\gamma(1+2\gamma)\mu_T}} = e^{-\gamma^2 \mu_T}.$$

This concludes the proof of the theorem. \square

EC.3. Bin Packing

Recall the online bin packing problem consists of placing jobs in unit-sized bins, where each job $j = 1, \dots, n$ has size V_j . Job size is unknown but follows a distribution μ . Jobs arrive in T batches of size q , so $n = Tq$.

Given a batch $V = \{V_1, \dots, V_q\}$ of q jobs and a corresponding assignment $x_1, \dots, x_q \in \{1, \dots, m\}$, we denote by $\text{size}_i(x, V) := \sum_{j: x_j = i} V_j$ the total size of jobs assigned to bin $i = 1, \dots, m$. Given assignments x^1, \dots, x^{t-1} for the first $t - 1$ batches, with job sizes stored in vectors V^1, \dots, V^{t-1} , and a sequence of batches $\tilde{V}^t, \dots, \tilde{V}^T$ for the remaining rounds, we say that the assignments $\bar{x}^t, \tilde{x}^{t+1}, \dots, \tilde{x}^T$ are an *optimal extension* if (i) the complete assignment $x^1, \dots, x^{t-1}, \bar{x}^t, \tilde{x}^{t+1}, \dots, \tilde{x}^T$ is feasible for the batches $V^1, \dots, V^{t-1}, \tilde{V}^t, \dots, \tilde{V}^T$, i.e., $\sum_{\sigma=1}^{t-1} \text{size}_i(x^\sigma, V^\sigma) + \text{size}_i(\bar{x}^t, \tilde{V}^t) +$

$\sum_{\tau=t+1}^T \text{size}_i(\tilde{x}^\tau, \tilde{V}^\tau) \leq 1$ for all $i = 1, \dots, m$; and (ii) the assignment $x^1, \dots, x^{t-1}, \bar{x}^t, \tilde{x}^{t+1}, \dots, \tilde{x}^T$ uses as few bins as possible. We use $\text{OPT}(\tilde{V}^t, \dots, \tilde{V}^T | x^1, \dots, x^{t-1})$ to denote the total number of bins used by this optimal assignment. Finally, we use shorthand notation $x^{\leq t-1} = (x^1, x^2, \dots, x^{t-1})$.

As noted in the main text, we use here a slight modification of the SSOA algorithm, in which all uncertainty realizations are sampled at the beginning of the horizon, and therefore denoted by $\tilde{V}^1, \dots, \tilde{V}^T$. This is described in Algorithm 4.

Algorithm 4 SSOA algorithm for the stochastic bin packing problem.

Obtain sample path $\tilde{V}^1, \dots, \tilde{V}^T$ by sampling each batch (with q jobs) independently from μ .

for $t = 1, \dots, T$ **do**

Observe the current batch V^t .

Compute assignments $(\bar{x}^t, \tilde{x}^{t+1}, \dots, \tilde{x}^T)$ that form an optimal extension for $V^t, \tilde{V}^{t+1}, \dots, \tilde{V}^T$ given the current assignment $\bar{x}^1, \dots, \bar{x}^{t-1}$ of the batches V^1, \dots, V^{t-1} .

Use the assignment \bar{x}^t to assign the jobs of the current batch V^t .

end for

Theorem 2 *The SSOA algorithm returns a feasible solution to the stochastic bin packing problem. Assume that $\sqrt{q}(\log^{3/4} q) e^{c \cdot \log^{3/2} q} \geq n$, for a sufficiently small constant c . Then, the SSOA algorithm opens in expectation $\mathbb{E}(\text{OPT}) + \mathcal{O}\left(\frac{n \log^{3/4} q}{\sqrt{q}}\right)$ bins.*

The proof proceeds by tracking the evolution of the $\text{OPT}(\tilde{V}^t, \dots, \tilde{V}^T | \bar{x}^{\leq t-1})$, that is, of the cost estimate given that the algorithm has already made decisions $\bar{x}^{\leq t-1} = (\bar{x}^1, \bar{x}^2, \dots, \bar{x}^{t-1})$. When $t = 1$, this cost is $\text{OPT}(\tilde{V}^1, \dots, \tilde{V}^T | \emptyset)$, which is equal to the true optimum in expectation (since \tilde{V}^t and V^t have the same distributions). At time $t = T + 1$, this cost is $\text{OPT}(\emptyset | \bar{x}^{\leq T})$, which is the total cost of the algorithm over the true instance. Thus, to prove Theorem 2, it suffices to bound:

$$\text{OPT}(\tilde{V}^{t+1}, \dots, \tilde{V}^T | \bar{x}^{\leq t}) - \text{OPT}(\tilde{V}^t, \dots, \tilde{V}^T | \bar{x}^{\leq t-1}). \quad (\text{EC.22})$$

Consider a fixed round t . By the principle of optimality, the best extension of $\bar{x}^{\leq t-1}$ for the batches $V^t, \tilde{V}^{t+1}, \dots, \tilde{V}^T$ is the same as using the assignment \bar{x}^t for V^t and then computing an optimal extension for the remaining batches $\tilde{V}^{t+1}, \dots, \tilde{V}^T$. That is:

$$\text{OPT}(V^t, \tilde{V}^{t+1}, \dots, \tilde{V}^T | \bar{x}^{\leq t-1}) = \text{OPT}(\tilde{V}^{t+1}, \dots, \tilde{V}^T | \bar{x}^{\leq t}) \quad (\text{EC.23})$$

Thus, upper bounding the difference (EC.22) is equivalent to upper bounding

$$\text{OPT}(V^t, \tilde{V}^{t+1}, \dots, \tilde{V}^T | \bar{x}^{\leq t-1}) - \text{OPT}(\tilde{V}^t, \tilde{V}^{t+1}, \dots, \tilde{V}^T | \bar{x}^{\leq t-1}). \quad (\text{EC.24})$$

That is, given the decisions $\bar{x}^{\leq t-1}$, we need to show that the total cost is not significantly impacted whether the next batch of jobs is V^t or \tilde{V}^t . We leverage “coupling” between the jobs in V^t and \tilde{V}^t to design an assignment for V^t from an assignment for \tilde{V}^t . A crucial component in this process are *monotone matchings*, which only match two values if the second is at least as large as the first.

DEFINITION EC.3 (MONOTONE MATCHING). Given two sequences $a_1, \dots, a_n \in \mathbb{R}$ and $b_1, \dots, b_n \in \mathbb{R}$, a *monotone matching* π from the a_j ’s to the b_j ’s is an injective function from a subset $J \in \{1, \dots, n\}$ to $\{1, \dots, n\}$ such that $a_j \leq b_{\pi(j)}$ for all $j \in J$. We say that a_j is *matched* to $b_{\pi(j)}$ if $j \in J$, and *unmatched* otherwise.

Intuitively, thinking of a_1, \dots, a_n and b_1, \dots, b_n as sequences of jobs, a monotone matching indicates that, if job $b_{\pi(i)}$ is assigned to some bin, then we can replace it with job a_i without violating the bin’s capacity. In other words, we can use an assignment of the jobs b_1, \dots, b_n to come up with an assignment of the matched jobs in a_1, \dots, a_n using the same bins. A surprising result from [Rhee and Talagrand \(1993a\)](#) is that if the two sequences are sampled i.i.d. from the same distribution, then almost all items can be matched using a monotone matching (see the original paper for a more general statement).

Theorem 6 (Monotone Matching Theorem ([Rhee and Talagrand 1993a](#))) *Suppose the random variables A_1, \dots, A_n and B_1, \dots, B_n are all sampled independently from a distribution μ over $[0, 1]$. Then there is a constant c such that with probability at least $1 - e^{-c \log^{3/2} n}$ there is a monotone matching π of the A_i ’s to the B_i ’s where at most $c\sqrt{n} \log^{3/4} n$ of the A_i ’s are unmatched.*

Using this result we can upper bound the difference given in Equation ([EC.24](#)) as follows.

LEMMA EC.6. *There is a constant c such that with probability at least $1 - e^{-c \log^{3/2} q}$, we have*

$$\text{OPT}(V^t, \tilde{V}^{t+1}, \dots, \tilde{V}^T | \bar{x}^{\leq t-1}) - \text{OPT}(\tilde{V}^t, \tilde{V}^{t+1}, \dots, \tilde{V}^T | \bar{x}^{\leq t-1}) \leq c\sqrt{q} \log^{3/4} q.$$

Proof. Let V_1^t, \dots, V_q^t be the realized item sizes in the t -th batch, and $\tilde{V}_1^t, \dots, \tilde{V}_q^t$ be the sampled item sizes in the t -th batch. Let $\tilde{x}^t, \dots, \tilde{x}^T$ be the optimal assignment extension for the batches $\tilde{V}^t, \dots, \tilde{V}^T$ given the previous assignments $\bar{x}^{\leq t-1}$, so that the assignment $\bar{x}^{\leq t-1}, \tilde{x}^t, \dots, \tilde{x}^T$ of the batches $V^1, \dots, V^{t-1}, \tilde{V}^t, \dots, \tilde{V}^T$ uses $\text{OPT}(\tilde{V}^t, \dots, \tilde{V}^T | \bar{x}^{\leq t-1})$ bins.

We map this assignment into an assignment for the jobs $V^1, \dots, V^{t-1}, V^t, \tilde{V}^{t+1}, \dots, \tilde{V}^T$, using a monotone matching. In this sequence, the t -th batch has been changed from the sampled sizes to the realized sizes. Let π be a monotone matching from V_1^t, \dots, V_q^t to $\tilde{V}_1^t, \dots, \tilde{V}_q^t$, given by [Theorem 6](#). Then define the assignment \hat{x}^t of the jobs in the t -th batch V^t as follows: (i) if V_j^t is matched by π , then assign it to the bin where $\tilde{V}_{\pi(j)}^t$ was assigned to by \tilde{x}^t , i.e., $\hat{x}_j^t = \tilde{x}_{\pi(j)}^t$; and (ii) otherwise, place job j in a new bin by itself.

First, $\bar{x}^{\leq t-1}, \hat{x}^t, \tilde{x}^{t+1}, \dots, \tilde{x}^T$ is a valid assignment of the batches $V^1, \dots, V^{t-1}, V^t, \tilde{V}^{t+1}, \dots, \tilde{V}^T$. Clearly, the capacity constraint is satisfied for all newly opened bins. For any other bin i , we know that $\text{size}_i(\hat{x}^t, V^t) \leq \text{size}_i(\tilde{x}^t, \tilde{V}^t)$, since the assignment \hat{x}^t replaces each item from \tilde{V}^t by a smaller item from V^t , due to the monotone matching. Thus, the total size in bin i is

$$\begin{aligned} & \sum_{\sigma=1}^{t-1} \text{size}_i(\bar{x}^\sigma, V^\sigma) + \text{size}_i(\hat{x}^t, V^t) + \sum_{\tau=t+1}^T \text{size}_i(\tilde{x}^\tau, \tilde{V}^\tau) \\ & \leq \sum_{\sigma=1}^{t-1} \text{size}_i(\bar{x}^\sigma, V^\sigma) + \text{size}_i(\tilde{x}^t, \tilde{V}^t) + \sum_{\tau=t+1}^T \text{size}_i(\tilde{x}^\tau, \tilde{V}^\tau) \\ & \leq 1. \end{aligned}$$

Moreover, the number of bins used by the new assignment $\bar{x}^{\leq t-1}, \hat{x}^t, \tilde{x}^{t+1}, \dots, \tilde{x}^T$ is at most the number of bins used by the old assignment $\bar{x}^{\leq t-1}, \tilde{x}^t, \dots, \tilde{x}^T$ plus the number of new bins opened, equal to the number of unmatched jobs in V^t . From Theorem 6 the number of unmatched jobs is at most $c\sqrt{q}\log^{3/4}q$ with probability at least $1 - e^{-c\log^{3/2}q}$. Therefore, with probability at least $1 - e^{-c\log^{3/2}q}$, the number of bins used by the new assignment is at most

$$\text{OPT}(\tilde{V}^t, \dots, \tilde{V}^T \mid \bar{x}^{\leq t-1}) + c\sqrt{q}\log^{3/4}q.$$

This concludes the proof of the lemma. \square

Proof of Theorem 2. By taking a union bound, Lemma EC.6 holds for all $t = 1, \dots, T$ with probability at least $1 - Te^{-c\log^{3/2}q}$. Under such event, using Equation (EC.23) we have

$$\begin{aligned} \text{OPT}(\tilde{V}^{t+1}, \dots, \tilde{V}^T \mid \bar{x}^{\leq t}) &= \text{OPT}(V^t, \tilde{V}^{t+1}, \dots, \tilde{V}^T \mid \bar{x}^{\leq t-1}) \\ &\leq \text{OPT}(\tilde{V}^t, \tilde{V}^{t+1}, \dots, \tilde{V}^T \mid \bar{x}^{\leq t-1}) + c\sqrt{q}\log^{3/4}q \end{aligned}$$

Telescoping this inequality over $t = 1, \dots, T$, we obtain:

$$\text{OPT}(\emptyset \mid \bar{x}^{\leq T}) \leq \text{OPT}(\tilde{V}^1, \dots, \tilde{V}^T \mid \emptyset) + cT\sqrt{q}\log^{3/4}q.$$

Recall that $\text{OPT}(\emptyset \mid \bar{x}^{\leq T})$ is the cost of our SSOA algorithm, denoted by ALG, and that $\text{OPT}(\tilde{V}^1, \dots, \tilde{V}^T \mid \emptyset)$ is the offline optimum. Thus, with probability at least $1 - Te^{-c\log^{3/2}q}$, we have:

$$\text{ALG} \leq \text{OPT} + cT\sqrt{q}\log^{3/4}q.$$

Let G be the event that this inequality holds, and let G^c be its complement. Since the algorithm always uses at most n bins, we obtain:

$$\begin{aligned} \mathbb{E}(\text{ALG}) &= \mathbb{E}(\text{ALG} \mid G) \Pr(G) + \mathbb{E}(\text{ALG} \mid G^c)(1 - \Pr(G)) \\ &\leq \mathbb{E}(\text{OPT} \mid G) \Pr(G) + n(1 - \Pr(G)) + cT\sqrt{q}\log^{3/4}q \\ &\leq \mathbb{E}(\text{OPT}) + cT\sqrt{q}\log^{3/4}q + nTe^{-c\log^{3/2}q}. \end{aligned}$$

Finally, the assumption on q guarantees that $ne^{-c\log^{3/2}q} \leq \sqrt{q}\log^{3/4}q$, so the expected cost of the algorithm is at most $\mathbb{E}(\text{OPT}) + \mathcal{O}(T\sqrt{q}\log^{3/4}q)$. We conclude by leveraging the fact that $T = \frac{n}{q}$.